Scaling and systems biology for integrating multiple organs-on-a-chip

John P. Wikswo* [a,b,c], Erica L. Curtis,[a,b] Zachary E. Eagleton,[a,b] Brian C. Evans,[a,b] Ayeeshik Kole,[a,b] Lucas H. Hofmeister,[a,b] and William J. Matloff[a,b]

Received (in XXX, XXX) Xth XXXXXXXXX 20XX, Accepted Xth XXXXXXXXX 20XX
DOI: 10.1039/b000000x

Coupled systems of *in vitro* microfabricated organs-on-a-chip containing small populations of human cells are being developed to address the formidable pharmacological and physiological gaps between monolayer cell cultures, animal models, and humans that severely limit the speed and efficiency of drug development. These gaps present challenges not only in tissue and microfluidic engineering, but also in systems biology: how does one model, test, and learn about the communication and control of biological systems with individual organs-on-chips that are one-thousandth or one-millionth of the size of adult organs, or even smaller, *i.e.*, organs for a milliHuman (mHu) or microHuman (μHu)? Allometric scaling that describes inter-species variation of organ size and properties provides some guidance, but given the desire to utilize these systems to extend and validate human pharmacokinetic and pharmacodynamic (PK/PD) models in support of drug discovery and development, it is more appropriate to scale each organ functionally to ensure that it makes the suitable physiological contribution to the coupled system. The desire to recapitulate the complex organ-organ interactions that result from factors in the blood and lymph places a severe constraint on the total circulating fluid (~ 5mL for a mHu and ~5μL for a μH) and hence on the pumps, valves, and analytical instruments required to maintain and study these systems. Scaling arguments also provide guidance on the design of a universal cell-culture medium, typically without red blood cells. This review presents several examples of scaling arguments and discusses steps that should ensure the success of this endeavour.

[a]Introduction

Organ-on-chip (OoC) microphysiological systems (MPS) programs funded by a variety of governmental agencies in the United States, Europe, and Asia are developing individual organs-on-a-chip and, more important, coupling human-cell, multi-organ, organ-on-chip and larger human organ construct (HoC) systems for drug development and studies of drug toxicity and efficacy. While individual OoC technologies have advanced considerably in the past decade,[1-6] significant technical challenges must be met before multiple organs can be integrated into a single system of coupled organs.[1] Only limited reports describe coupled organs,[2;3] and there is not yet a full understanding of how biological scaling laws apply to multiple, coupled OoCs. To replicate human physiology and drug response with interconnected human OoCs/HoCs, it is critical that each OoC/HoC has the correct relative size. Extensive literature describes differences in organ size between animal species whose body mass, M_b, spans 6 orders of magnitude from shrew to whale. Organ size does not scale proportionally (isometrically) with M_b, but instead obeys a number of different allometric power laws that describe, for example, how as the animal's linear dimension L increases, its mass increases as L^3, and hence the cross-sectional area of the bones must increase non-linearly.[4] Metabolic rates may exhibit $M_b^{3/4}$ scaling,[5-8] pulmonary and vascular networks exhibit $M_b^{3/4}$ scaling,[9;10] and blood circulation time scales as $M_b^{1/4}$.[11] Table 1 shows the coefficients A and B, derived from primates with body masses of 10 g to 100 kg,[12] to compute organ mass $M = AM_b^B$. When multiple organs are connected, their relative size could be normalized to mass, surface area, volumetric flow, or other geometric measures. The challenge is to specify the appropriate scaling law(s) for specific applications, whether it be to construct a physically functional organ (*e.g.*, a pumping heart), a pharmacodynamic model (3D co-culture systems), or both simultaneously in a MPS.

For convenience we select three scales for our discussion: Human (Hu), milliHuman (mHu), and microHuman (μHu); we assume an adult Hu mass of 70 kg and hence a mHu mass of 70 g and a μHu mass of 70 mg. In theory, a system with multiple organs could be designed to represent any fraction of a human, possibly a nanoHuman (nHu). In this paper we discuss the factors that guide the specification of the size of each organ in a coupled system. We hope that this will provide guidance to the ongoing efforts to design and implement coupled organ systems.

Allometric scaling

i. Principle

Allometric scaling has been of great academic interest, but it is largely unexplored in the design of coupled microphysiological systems. As reviewed elsewhere,[1] allometric scaling formed the early foundation of pharmacokinetic modeling of the delivery and activity of a drug within a human relative to experiments using culture dishes and small mammals, but it has been supplanted by scaling based upon physiology rather than simply mass or body surface area.[13-15]

[a] *Vanderbilt Institute for Integrative Biosystems Research and Education, Vanderbilt University, Nashville, TN 37235, USA. Fax:1-615-322-4977; Tel: 1-615-343-4124. E-mail: john.wikswo@vanderbilt.edu*
[b] *Department of Biomedical Engineering, Vanderbilt University, Nashville, TN 37235, USA*
[c] *Department of Molecular Physiology & Biophysics and Department of Physics & Astronomy, Vanderbilt University, Nashville, TN 37235, USA*

ii. Pros/cons

In this review, we follow a similar trajectory, beginning with simple allometric scaling to estimate organ size, and then concluding that the requisite OoC and HoC scaling must reflect physiological activity and the efficiency with which engineered tissues can replicate human organ function *in vivo*. The power of allometric scaling is that there is a rich literature to guide the OoC/HoC designer, as provided in the Scaling Spreadsheet in the Electronic Supplementary Information (ESI). As we will show, allometric scaling provides an excellent starting point for specifying and validating coupled OoC/HoC systems.

However, this scaling may not produce valid parameters for mHu and μHu systems. The most notable observation from Table 1 is that the large human brain size (a=85) and its allometric scaling exponent (b=0.66) would produce a μBrain that has twice the body mass of the μHuman. The nature of this problem can be seen in Fig. 1. The intersections of the allometric scaling lines for each organ with the vertical mHu and μHu lines in Fig. 1A indicate the allometric mass of the mHu and μHu organ in Table 1. The scaling of each organ relative to its mass for a 1.0 Hu is shown in Fig. 1B, which suggests that allometric scaling for the brain, pituitary, adrenals, and thyroid will produce larger than average organs, while that for the thyroid will be smaller. Given its median position, one might consider using the pancreas scaling as a starting point, with $B = 0.91$.

Table 1 Allometric scaling coefficients and organ masses for a Hu, mHu, and μHu based upon primate data. Coefficients from Stahl, 1965.[12]

			Human		milliHuman (mHu)		microHuman (μHu)		Relative Organ Mass Ratios	
Organ	A	Body mass: B	60 kg M, g	Organ / Body	60 g M, g	Organ / Body	60 mg M, mg	Organ / Body	M_{mHu}/M_{Hu}	$M_{\mu Hu}/M_{Hu}$
Liver	33.2	0.93	1496	2.5%	2.4	4.0%	3.9	6.6%	1.62E-03	2.63E-06
Brain	85	0.66[a]	1268	2.1%	13	22%	139	232%	1.05E-02	1.10E-04
Lungs	9.7	0.94	455	0.76%	0.69	1.2%	1.0	1.7%	1.51E-03	2.29E-06
Heart	5.2	0.97	276	0.46%	0.34	0.57%	0.42	0.70%	1.23E-03	1.51E-06
Kidneys	6.3	0.87	222	0.37%	0.54	0.91%	1.3	2.2%	2.45E-03	6.03E-06
Pancreas	2.0	0.91	83	0.14%	0.15	0.26%	0.29	0.48%	1.86E-03	3.47E-06
Spleen	1.5	0.85	49	0.081%	0.14	0.23%	0.39	0.64%	2.82E-03	7.94E-06
Thyroid	0.15	1.12	15	0.025%	0.0064	0.01%	0.0028	0.0047%	4.37E-04	1.91E-07
Adrenals	0.53	0.7	9.3	0.016%	0.07	0.12%	0.59	0.98%	7.94E-03	6.31E-05
Pituitary	0.03		0.49	0.00081%	0.0044	0.0074%	0.040	0.067%	9.12E-03	8.32E-05

[a] Coefficients for human brain scaling: 80-90. The corresponding number for monkeys is 20-30, and great apes 30-40.

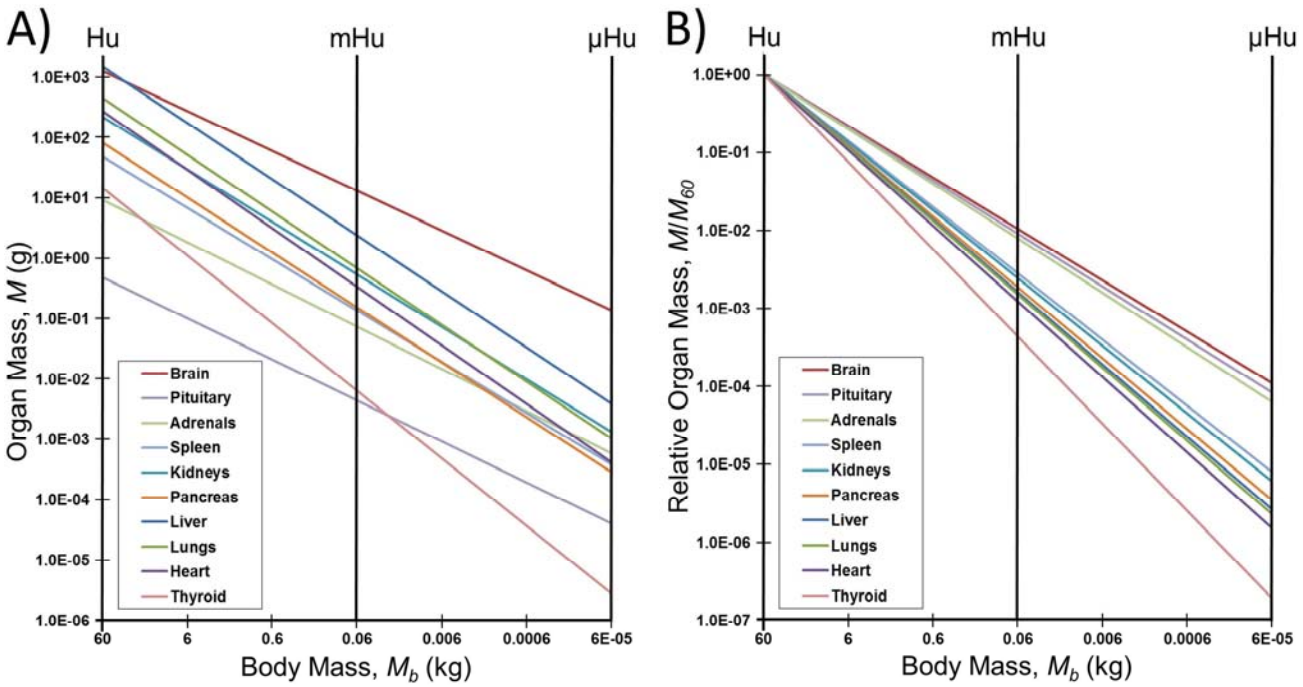

Fig. 1 How allometric scaling might (mis)inform mHu and μHu scaling when known power laws[12] are used to extrapolate from humans. A) Organ mass in grams. B) The mass of each organ relative to that for a 1.0 Hu. Note the range in allometric slopes for different organs, and that a 10^6 reduction in body mass leads to only a 10^4 reduction in the mass of the brain, pituitary, and adrenals, leading to a μBrain with twice the mass of the μHuman.

There would be similar issues were allometric scaling used to set the heart rates and blood circulation times. The heart rate of a mouse is approximately one hundred times that of an adult human,[11] and hence one would not want to assemble a mHu whose organs and the connecting vasculature would require perfusion at rates that would not be realistic for a human. Human

cells might not function properly or for long when placed in organs sized to a mouse.

Simple scaling will also fail for other reasons. A working heart cannot be less than one cardiomyocyte thick. Key endothelial layers must be one cell thick, and only one cell, independent of organ size. Certain immune cells function at such a low density (3,000 leukocytes per ml of cerebral spinal fluid (CSF)) that the breadth of acquired immune response may not be replicable in a μBrain with a CSF volume of ~ 1 μL that would contain about 3 leukocytes. Cellular heterogeneity should not scale.

Interconnected "histological sections"

i. Principle

Given that cells in OoCs/HoCs may not operate with the same efficiency as cells *in vivo*, it may be more realistic to construct an OoC/HoC system that reflects a small fraction of an adult human. Don Ingber has described this as creating "living histological 'sections' of an adult human" (personal communication).

ii. Pros/cons

This approach is ideal for OoC/HoCs operated in isolation, in that it effectively avoids the need for scaling by simply observing a small portion of an organ. The rate of perfusion can be determined by the number of cells being supported and the section can be studied for as long as it survives. The first challenge occurs if the media is recirculated – what is the correct volume for that media? The rate at which the OoC/HoC consumes nutrients, secretes metabolites, and otherwise conditions that media is determined by this volume, and to overestimate the volume might lead to proportion delays in the appearance, for example, of toxic metabolites, particularly if they have only limited lifetimes. It is necessary, however, to make the "section" large enough and sufficiently realistic that the organ functions in a more physiologically realistic manner than a simple monolayer monoculture in a Petri dish or well plate. Building a functional "section" from an individual human's cells may have advantages over using real ones[16] in that it may be possible to create "sections" of an individual patient's organs that are not readily available.

This approach is advantageous when one desires to recapitulate only a subset of an organ's function, for example, a lung alveolus with epithelial, endothelial, immune, and mechanical interactions but without requiring gas transfer,[17;18] a heart-on-a-chip that elucidates drug effects on cardiac electrophysiology or mechanical activity but doesn't pump blood,[19;20] or a gut-on-a-chip that does not consider bile activity, nutrient and water uptake, or abluminal transport.[21] In this case, the system may scale linearly, and in effect one is creating a local system with inputs, outputs, and selected physiological controls.[22]

However, the situation becomes more complex when two or more "histological sections" are coupled in series or parallel. Correct representation of organ-organ interactions is now determined by the size of each section and the volume of their shared fluid. A scaling mismatch of the two organs could make one section either oblivious of the other or dominated by it. Too large a fluid volume would delay or minimize organ-organ interactions. Furthermore, a small histological section may not be representative of the complexity of the organ as a whole and may be missing essential biological features that can alter biological responses to stimuli.

However, engineering all *in vivo* conditions artificially would fundamentally eliminate the need to couple the organ systems, and the same results could be achieved by running each organ in its own microenvironment. This contradicts the purpose of coupling the organ systems together, in which the goal is to observe the most physiologically accurate response and intra-organ signaling to perturbations in the system without *a priori* biases. Hence we need functional scaling of our "sections."

Functional Scaling

i. Principle

Given the shortcomings of allometric scaling and the uncertainties of how to scale coupled "histological sections," it is worthwhile to examine the obvious alternative: functional or physiological scaling of coupled organs. With this approach, one identifies the organ functions that are the most important for the coupled system, *e.g.,* heart: volume pumped; lung: gas exchanged; liver: metabolism; kidney: molecular filtering and transport; brain: blood-brain barrier function and synapse formation. The functional parameters to be achieved for a particular implementation are specified, and then the physical milli- or micro-organ is sized, iteratively if necessary, to achieve the requisite functional activity given the constraints imposed by physical architecture, materials, and available cells.

ii. Pros/cons

This is a rational approach to preserve specific organ functions at their appropriate relative magnitudes, rather than relying on the classical, allometric approach. Given that the chosen functions should be quantifiable, this provides a straightforward approach to designing both the device and the functional readouts of a complete OoC system.

One limitation of the approach is that functional scaling may result in oversimplification of OoCs and limit the translatability of the results achieved. Another is that it may not be possible to create an organ that recapitulates more than one organ function. Just as we saw in Fig. 1, different functions may scale differently with respect, for example, to surface-volume ratio. One could devise two-part organs, *e.g.,* a heart with separate chambers for recapitulating mechanical and electrophysiological functions. [19;20]

iii. Example

Figure 2 shows an example of a coupled mHu HoC system currently under development by a collaboration between Los Alamos National Laboratory, Vanderbilt University, the University of California San Francisco, Charité Hospital Berlin, Harvard University, and the CFD Research Corporation.[23] The design challenges are to properly size all organs to provide realistic organ-organ interactions, including drug metabolism, and to do so with a low enough volume of blood surrogate that the autocrine and paracrine signaling factors released by each organ are not diluted to below the level of physiological effect for other organs. A working heart and a functional lung are desired. Simple scaling would suggest that given an adult blood volume of ~4.5 liters, a mHu and a μHu would have blood volumes of ~4.5 ml and ~4.5 μl, respectively. A microfluidic cardiopulmonary assist system might be required as the system is assembled and the organs grow and stabilize, *e.g.,* if the lungs and heart have not yet achieved their needed level of gas exchange and pumping. Given that every organ in the body is not being represented, it may be necessary to include a microformulator[1;24;25] to add missing blood

components, as well as a means to neutralize ones that are not removed by a missing organ. Finally, in recognition that complex biological systems tend to oscillate, a system for sensing and control[22;26] will be required to maintain organ stability and simulate aspects of neurohumoral physiological control not explicitly included, thereby ensuring both homeostasis and the requisite physiological daily and longer biorhythms.

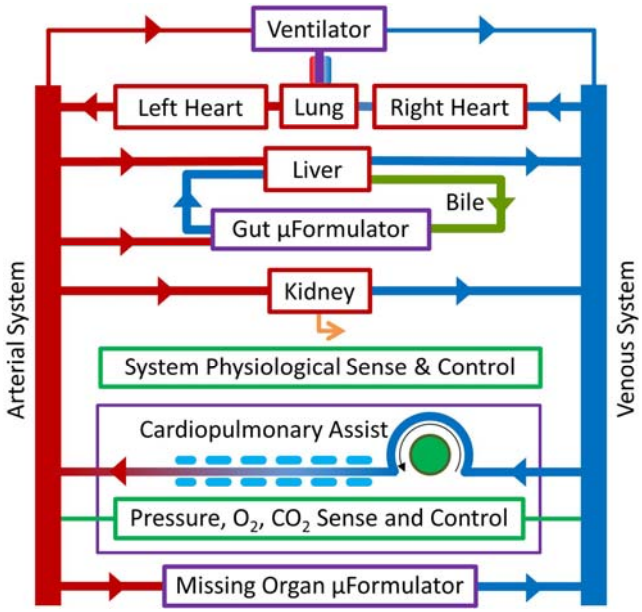

Fig. 2 The mHu Advanced Tissue-engineered Human Ectypal Network Analyzer (ATHENA), a milliHuman (*Homo chippus)* being developed by Los Alamos National Lab, Vanderbilt University, Charité Universitätsmedizin Berlin, University of California – San Francisco, Harvard University, and CFD Research Corporation with the support of the Defense Threat Reduction Agency (DTRA).[23] Figure from Wikswo *et al., 2013,* with permission.[1]

Examples of organ scaling

We now present several examples of scaling considerations that might apply to the creation of individual organs. In the ESI Scaling Spreadsheet, we present an extensive compilation, with appropriate references from a vast and often inconsistent literature, of ~250 anatomical and functional parameters for the brain, heart, kidney, liver, lung, and blood that can be used to guide the design, modeling, and validation of OoCs and HoCs, using either allometric or functional scaling. In the following paragraphs we provide a brief discussion of the importance of several of the parameters for each organ.

Our examples are limited to the major organs that are common therapeutic targets and do not include other significant tissues such as adipose, bone, endocrine, skeletal muscle, or skin tissues. When attempting to recapitulate *in vivo* metabolic and physiologic demands of a coupled organ system, one must consider that these tissues also play a key role in metabolic demands and biochemical signaling. As a result, design criteria for OoC scaling should take into consideration the presence, absence, and simulation of various organs when scaling certain physiologic parameters. The ESI Scaling Spreadsheet and the discussion of each example below should provide guidelines for a rational approach to the design of integrated HoC/OoC systems.

Brain

There are a growing number of reports on *in vitro*, flow-based models of the neurovascular unit (NVU) and blood-brain barrier (BBB),[27-31] and other neural co-cultures.[32-35] For this scaling analysis, we choose to reduce the brain from its extreme structural and functional complexity and focus our analysis on scaling of the NVU, which is the most important functional unit for ADMET (absorption, distribution, metabolism, and excretion toxicity) studies and functionally represents the BBB. The NVU consists of a capillary and its surrounding cell types, including endothelial cells, pericytes, astrocytes, microglia, and neurons. Correct and, importantly, feasible scaling of an NVU will require a unique combination of geometrical and biochemical scaling.

This is important because the brain is particularly complex, and the literature is riddled with inconsistent physiological data. For example, one of the most common misconceptions of brain physiology is that glial cells outnumber neurons by ten to one, where in fact the ratio for neocortical glia to neurons is 1.2, and the ratio of non-neuronal to neuronal cells ranges from 0.2 to 1.5, depending upon the brain region. These ratios are of exquisite importance when constructing a brain-on-a-chip.

Many of these misconceptions arise from the difficulty of studying the brain. Brain tissue is very diverse across species, and therefore studying the physiological parameters of rodent or other brains will not give an accurate representation of human physiology. The best understanding we can gain from non-human studies comes from the primate brain. The architectural complexity of the brain also complicates the analysis of simple parameters such as capillary density and cell numbers. Neurons can traverse multiple brain regions. Significant advances have been made in this regard by Herculano-Houzel *et al*., with their isotropic fractionator technique,[36] and improvements will continue to be made with more advanced analytical techniques such as the transparent brain recently developed by Chung *et al*.[37]

As the ESI Scaling Spreadsheet indicates, gray matter and white matter may also contain different ratios of cell types and orientations. These parameters are important for scaling in brain region-specific ways. The task of assembling these parameters is complicated because most groups studying the brain make empirical measurements on a specific brain region and not the whole-brain scale. In addition, metabolic parameters such as oxygen consumption are difficult to measure for specific brain regions, but capillary density and cell number distribution are far easier to measure for isolated brain regions. To further complicate gathering this information, many of these parameters had to be assembled by studying the control groups from manuscripts investigating a specific disease state. Finally, it is unclear which of these parameters will be most important for the end goal of creating and integrating a brain-on-a-chip. Therefore, in the Scaling Spreadsheet we present our best understanding of the necessary physiological parameters and their sources for the reader to evaluate and employ as necessary. We envision this table of parameters as evolving as alongside our understanding of the human brain and the challenges of building HoCs.

Functional scaling of the brain is largely driven by metabolism. In humans the brain represents 20% of the overall metabolic load and 2% of overall body mass.[38;39] Moreover, the relative metabolic demand of the brain grows more slowly than

body and brain mass (allometric exponent 0.873).[40;41] The total energy consumption by the brain varies linearly with the number of neurons in the brain at a rate of 5.79×10^{-9} μmol glucose·min^{-1}neuron^{-1}.[40] However, it is unclear if an *in vitro* brain-on-a-chip (BoC) can recapitulate the metabolic rate of the *in vivo* case. Therefore, we believe that a mHu and μHu BoC, for example, should be scaled linearly by the number of neurons in the adult human brain, and the remaining components of the brain should be scaled according to the metabolic demand of the number of neurons in the BoC. Autoregulation of the BBB by all cellular components of the NVU also necessitates correct scaling of the cell numbers in the BoC and capillary surface areas in relation to the metabolic demand of the neurons which they support. According to the cellular composition of the cerebral cortex, the NVU should consist of 1.2 astrocytes/neuron, 0.46 vascular cells/neuron, and 0.2 microglia/neuron.[42]

The greatest challenge in geometrical scaling of the brain is realization of the capillary density of the brain, which has one of the largest capillary densities of any organ. The average human adult has between 12 and 18 m^2 of BBB, or 150 to 200 cm^2g^{-1} of tissue. The necessity of providing neurons with such a high capillary surface area per neuron (174 $\mu m^2 neuron^{-1}$) will challenge fabrication techniques and is most feasible in microfluidic systems.[42;43] In association with the vasculature, pericytes cover around 30% (5 m^2, 667 cm^2g^{-1}) and astrocytes cover around 99% (18 m^2, 200 cm^2g^{-1}) of the abluminal surface of brain microvasculature.[44-46]

Scaling of blood flow in a BoC relative to other OoCs could present significant challenges. The human brain has a flow rate of 7 L·min^{-1}, which accounts for 13% of total blood flow.[47-50] This number should scale functionally with the size and metabolism of the BoC in order to supply sufficient glucose, oxygen, and other nutrients and remove resulting metabolites. Values such as the central metabolic rate for oxygen (CMRO2) of 3.2 mL/100 g·min should remain constant with decreased size and will be a useful readout of BoC success.[47] Another critical factor is maintenance of the shear stress at the endothelial barrier. Blood surrogate flow must be supplied to a BoC with a sufficiently small capillary cross-sectional area to maintain a shear of around 1.5 Pa without excessive volumetric flow rates.[51-53] This value will also determine the pharmacokinetic parameters of the brain by influencing the residence time and Péclet number of the BoC capillaries.

In summary, the scaling of a BoC revolves around the NVU and is focused on delivering the correct metabolic demand relative to other organs and the unique transport properties of the BBB. As these technologies develop it will become more clear which of these scaling laws are critical to success, and also where scaling can or must be broken in favor of realistic implementation of these technologies for routine studies.

Heart

The scaling considerations that apply to the development of heart tissue revolve around tissue architecture and composition, electrical conduction, biochemical factors, metabolism, and fluid flow. An important decision that must be addressed early in the development of an OoC/HoC heart is whether it is to be a working heart, *i.e.*, support the flow of blood against a mechanical load (including the pulmonary or peripheral vasculature),[54-58] or serve as an electromechanical sensor of the effects of drugs and their metabolites on cardiac performance.[19;20]

The cardiac parameters in the ESI Scaling Spreadsheet support several of the major cardiac scaling issues we have discussed. For example, if a heart construct is to be used as the fluidic pump that provides and supports circulation of a blood surrogate through a coupled OoC system, then functional parameters such as transport capacity, ejection fraction, and fractional cell shortening become scaling issues of paramount importance. The ESI Scaling Spreadsheet is constructed to circumvent the need to look up individual organ parameters, which often vary throughout the literature and species type. Furthermore, a desired organ size can be used to quickly calculate approximate parameter values for an organ of a certain size based upon both allometric and functional scaling. Thus the table is a valuable resource for quickly and efficiently approximating functional and structural parameters for OoC design, and it also highlights a number of the scaling issues that must be considered in terms of design criteria.

Composition and biochemical factors are of significant import in modeling mammalian heart tissue, which is intrinsically heterogeneous, containing cardiomyocytes, fibroblasts, vascular smooth muscle cells, endothelial cells, and neuronal cells among other less abundant non-myocytic cells.[59] These cell types all interact through a variety of biochemical factors and signaling mechanisms to maintain cardiomyocyte phenotype and tissue function.[60-65] In terms of these fundamental signaling pathways, one may need to consider exogenous sources of biochemical factors that are scaled to the targeted tissue construct's mass, volume, and composition. One must also consider that the size of the organ construct will limit the ability to accurately recreate features of the mammalian heart (*e.g.*, if the size of a heart construct is limited to 1-2 cells thick, as would be required for a μHeart, then the realization of an endocardium and the incorporation of all native cell types will not be feasible), whereas this might be possible with a 15-myocyte thick mHeart.

Tissue architecture and metabolism must also be considered. The specialized cells that comprise heart tissue are organized in a highly specific structure that results in a transendothelial biochemical gradient that forms the blood-heart barrier. Furthermore, the fibers in the heart are aligned in anisotropic, helically wound layers that impart unique, spatiotemporally dynamic biomechanical properties to heart tissue. This issue is of key importance when considering the use of a scaffold or substrate as a culture platform, since mismatched substrate and tissue properties can result in a significant reduction in cardiac pump function. In addition to its complex architecture, heart tissue is very metabolically active and requires sufficient oxygenation. Thus, scaling cellular metabolism is another concern, as the balance of energy supply and demand is essential for maintaining cardiac pump function. To meet this demand, native heart tissue contains a dense, complex network of myocardial capillaries that penetrate orthogonally through the myocardium. However, recapitulating a complex network of small diameter capillaries may not yet be feasible *in vitro*, although recent developments are promising.[66;67] As a result, the utilization of planar diffusion may suffice for now, as the reduced thickness of the cultured myocardium of engineered heart tissue may allow for adequate oxygenation without vascular perfusion.

Fluid flow and other biomechanical stimulation of cardiac tissue are integral to a variety of the heart's intrinsic control mechanisms. Synchronized cardiomyocyte contraction results in complex mechano-electrical feedback mechanisms through the activation of stretch-activated channels and modulation of cellular calcium handling, the endocardium responds to both fluid shear stresses and pulsatile cyclical strain by releasing paracrine and endocrine factors, and baroreceptors transduce sensory feedback into various forms of cellular signaling. Under normal fluid shear conditions, endothelial and vascular smooth muscle cells have relatively low rates of proliferation, whereas abnormal hemodynamic conditions result in pathological cellular phenotypes that are associated with a number of cardiovascular diseases.[68] The proper scaling of biomechanical properties in conjunction with fluid dynamics is therefore crucial to modeling both normal and pathological cardiac tissue. In order to achieve physiologic fluid shear stresses in miniaturized working heart constructs, one must appropriately apply volumetric and resistance scaling by modulating flow rates and blood surrogate/media viscosity in accordance with the geometry of the bioreactor and tissue construct. These scaling issues only gain significance when integrating heart-on-a-chip technologies into multi-organoid constructs, especially if the heart tissue is to be responsible for cardiac output to perfuse the entire organ network. Here, cardiac output (*i.e.,* stroke volume, heart rate, ejection fraction, etc.), tissue size, metabolic and perfusion demands of other tissues, total peripheral resistance, and resident blood surrogate volume are all variables that need to be properly scaled relative to each other. However daunting it may be, the scaling of biological variables for the integration of multiple human organ constructs provides a basis for fabricating functional mHu or μHu constructs that would streamline drug development and discovery and produce a more realistic cellular microenvironment than monolayer monocultures in Petri dishes or well plates.

Overall, each of these scaling issues merits consideration in the design of engineered heart constructs, and optimization of heart-on-a-chip technologies, not to mention all organ-on-a-chip technologies, is a compromise between verisimilitude and a functional abstraction.

Kidney

Building an *in vitro* kidney model necessitates architectural, functional, and biochemical scaling. The nephron consists of three structurally and functionally distinct subunits–glomerular filtration, proximal reabsorption and secretion, and urine concentration–which must scale individually as well as relative to one another in order to preserve whole organ functionality.

The ESI Scaling Spreadsheet provides examples and literature references for a range of functional and structural factors that need to be considered in kidney scaling. First and foremost, the kidney model must scale in order to sufficiently filter the circulating volume of blood in the HoC construct and achieve physiologically relevant rates of the glomerular filtration. Second, the model must be manipulated to facilitate physiological rates of fractional reabsorption, a challenging feat due to the wide discrepancies between *in vivo* functionality and *in vitro* performance. The kidney also provides a unique example of an organ in which the preservation of geometrical features, such as the countercurrent mechanism and exchanger, is critical to realizing an accurate model of the human kidney.

Functional scaling begins in the glomerulus. The glomerular filtration rate (GFR) in a 70 kg human produces 125 mL/min of ultrafiltrate and therefore 125 μL/min in a functional milliHuman (mHu).[39] The ratio of the surface area of the glomerular hemofilter to porous surface area can be optimized in the model to achieve this rate of filtration, given that a physical filter will be different from a biological one.

Recapitulation and subsequent scaling of the specific transport, metabolic, endocrine, and immune activities of the renal tubules pose formidable fabrication and scaling challenges.[69;70] A potential approach begins with functional scaling of active solute reabsorption rate in the proximal tubule. For example, a 70 kg human normally filters 180 g per day of D-glucose, almost all of which is reabsorbed in the proximal tubule; therefore, a mHu kidney must scale to filter and subsequently reabsorb about 180 mg of glucose per day.[71] Because metabolic activity and active transport abilities of the proximal cells *in vitro* may differ significantly from *in vivo* quantities, preliminary *in vitro* studies must be conducted to characterize the phenotype of human proximal tubule cells in single hollow fibers. From these results, we can predict the number of cells and surface area required for functional scaling of solute reabsorption. Manipulation of geometric dimensions or the use of parallel proximal tubule modules can ensure that the proximal tubule model can receive the appropriate volume of ultrafiltrate from the glomerular unit.

Although the scaling of the urine-concentrating mechanism must encompass functional scaling concepts, the approach must also pay particular attention to scaling the critical architecture of the loop of Henle. Although the relation of absolute loop length and urine-concentrating ability between species is highly debated, the creation of the corticomedullary osmotic gradient is unequivocally linked to active reabsorption of Na^+ as well as the complex geometry of the loop of Henle.[72;73] In an approach similar to that of the proximal tubule model, functional scaling in the loop of Henle can be achieved by scaling the rate of Na^+ reabsorption. Active reabsorption of Na^+ by Na/K-ATPase pumps located in the thick ascending limb of the loop of Henle (TAL) effectively drives the passive H_2O reabsorption in the descending limb. Additionally, the Na/K-ATPase pump has been extensively characterized and is tunable with a variety of solutes, hormones, and drugs, and therefore may serve as a point of modulation for scaling purposes.[74] Successful scaling may be impossible without the preservation of architectural features such as the countercurrent mechanism and exchanger. Computational modeling can be used to optimize the length and surface area to volume ratios needed to establish a physiologically relevant osmotic gradient for a human, 300 to 1200 mOsm regardless of size.[75] Additionally, "preconditioning" of long loops with short loops, as seen *in vivo* in a ratio of 85 short to 15 long in humans, may help to maximize urine-concentrating ability.[73,76]

The kidney is an excellent example of a key OoC/HoC design concept: while functional and biochemical scaling may provide the best approach to scaling a histological section of a human, some organ functionalities cannot be achieved without reproduction and scaling of certain physiological architectures.

Liver

The ESI Scaling Spreadsheet provides an overview of the

available allometric scaling laws for the liver and a basis from which we can evaluate parameters that will scale and those that will not.[77] Intuitively, we can identify certain parameters that will not scale. For example, cellular parameters such as sinusoidal endothelial cell (SEC) fenestration size will remain 100-1000 nm in diameter.[78] Additionally, hepatocyte density (1.39×10^8 cells/g liver), protein concentration (90 mg/g liver), and liver density (1.03 g·liver/mL) are not expected to show appreciable scaling in our milli/microliver.[39;79]

There are, however, central design parameters for which there are allometric scaling laws, but from which we can justifiably deviate for functional scaling. For functional scaling, we argue that the hepatic mass will not follow the allometric power law and instead represent $1/10^3$ or $1/10^6$ of what is found in a normal human. For example, although an allometric power law exists for oxygen consumption, we instead use functional scaling given that the metabolic demand per hepatocyte—approximately 0.3 to 0.9 nmol/sec/10^6 cells—will be equivalent in our scaled OoC.[80;81] The allometric value for oxygen consumption in the mHu (O_2=$0.035M_b^{0.69}$, with M_b in g, such that a 60 g mHu would have a hepatic oxygen consumption of 0.59 ml/min) underestimates consumption when compared to a functional proportion of a normal human (2.06 ml/min).[9] Note that if oxygen transport through the blood surrogate is insufficient, a system of hydrophobic hollow fibers could be used to increase the interstitial oxygen concentration without affecting interstitial or blood volumes, as has been done quite successfully for liver HoCs.[82;83]

In addition to proper oxygen delivery, there is also a need to seed the appropriate number of cells with sufficient exposure to a blood surrogate. *In vivo* hepatocytes sit adjacent to the 1.4 μm perisinusoidal space (*i.e.*, the space of Disse), which separates the hepatocytes from the sinusoidal capillary that averages 10 μm in diameter and 275 μm in length. Appropriate concerns are whether a longer and larger *in vitro* model of a hepatic sinusoid unit via hollow fiber (HF) bioreactors will affect nutrient delivery, create unwanted oxygen gradients, and/or add to necessary volume given the limitations of HF fabrication. Although the number of hepatocytes needed for a *functional* mHu is calculated to be $3x10^8$ cells, it is unclear if current HF technology can support this.[83-85] Neither 3-D, planar microfabricated, or hollow-fiber livers have yet achieved collection of bile, generated by the liver canaliculi, into bile ducts.

Validation of the milli- and microliver models will primarily occur via iterative *in vitro-in vivo* correlation of xenobiotic clearance. Several groups have conducted correlation studies, with a general belief that each drug compound, unsurprisingly, may have its own allometric power law across species (due to metabolic variations) and also a different scaling factor (due to assumptions made in their model such as diffusional barriers).[86-93] For example, Naritomi *et al.* found that they could predict human *in vivo* clearance rates of eight model compounds from human *in vitro* data by using an animal scaling factor ($Cl_{in\ vivo}/Cl_{in\ vitro}$) from either a rat or a dog. Scaling factors were similar across species for each of the eight compounds, but varied from 0.3 to 26.6-fold among the compounds.[89]

While this variation may prove to be troublesome in the analysis of unknown compounds during drug evaluation and discovery stages, awareness of the properly scaled input parameters and thorough analysis of a wide range of model compounds (*e.g.,* acetaminophen, diazepam) will assist in building predictive pharmacokinetic/pharmacodynamic (PK/PD) models of the OoC system.

Lastly, Boxenbaum notes in an early paper on allometric scaling of clearance rates that these models may not prove to be accurate, particularly at small masses, as the intercept of the allometric equation predicts a non-zero clearance rate at 0 g. This collapse of allometric theory at the micro- and milliscale gives credence to the necessity to scale based on organ function.[22]

Lung

Within the lung, the bronchial tree and the alveoli can be scaled separately. The main structures in the lung that do not scale with system size are the individual cell parameters, such as cell volume and radius. While one might not expect to scale the percent distribution of cells, this may be necessary if the efficiency of a particular cell type in a mHu or μHu differs from that in a Hu.

The ESI Scaling Spreadsheet provides a collection of both functional and structural lung variables. Inconsistencies between the allometric exponents show a disconnect between structure and function, illustrating a novel problem when constructing HoCs. As we have discussed, additional support systems, such as assistance from a microformulator, may be necessary to ensure the most accurate structure/function μLung construct incorporated onto a HoC. A robust table of scaling values is therefore a valuable reference tool when making the inevitable compromises while designing a coupled OoC system.

Allometric scaling in the bronchial region is found in the diameters of the trachea and bronchioles. Allometrically, the diameter of the terminal bronchiole scales with an exponent of 0.21, while the radius of the trachea scales with an exponent of 0.39. However, this presents a problem: allometrically scaled, a μHu would have a terminal bronchiole diameter of 30 μm , which is near the limit of current soft-lithographic microfabrication technology; were hollow fibers used for the larger bronchial tubes, with a minimum diameter of 200 μm, the microfluidic network would require approximately six binary splittings to achieve a 240 μm diameter. Either scaling laws must be broken or novel fabrication techniques[94] utilized to accommodate and create a viable μHu trachea/bronchi system.[9]

Allometric scaling in the alveoli is critical as well. The most important function of the alveolus is oxygenation, so scaling should be addressed to meet oxygenation needs, if required for the MPS. The critical parameter to be properly scaled is surface area, as it is the main component of Fick's law and governs diffusion capacity across the alveolar-capillary barrier. Pulmonary diffusing capacity (DL_{O2}) scales linearly with body mass with an exponent of ~1.[95] This means that the DL_{02} /body mass ratio is relatively constant in all mammals. Diffusing capacity is related to alveolar surface area, mean barrier thickness, and capillary blood volume, and the allometric coefficients are 0.95 for surface area, 0.05 for barrier thickness, and about 1 for capillary blood volumes.[95]

To replicate a μHu, alveolar diameter would be 21 μm –an order of magnitude less than the average 200 μm diameter of a human. The diameter of a type 1 epithelial cell is around 20 μm.

Thus any individual μHu alveolus would require only a single epithelial cell,[9;96] but the entirety of alveolae for a 0.1 μHu might well be modeled by a rectangular membrane of the appropriate area.[17;18]

Another scaling argument that should be considered is the mass-of-tissue to volume-of-media, in this case lung tissue volume to blood volume. Blood volume is linearly related to body mass in mammals (allometric exponent of 1). Thus scaling lung tissue surface area and blood substitute volume in the HoC depends on the total mass of the system, and if both are scaled correctly then oxygen concentration should be sufficient. If scaling is ignored, problems could arise with the surface area required to supply the blood with sufficient oxygen for metabolic needs.[95]

A μLung would have 184,000 cells in the alveolar region. Around 37% of those (the interstitial cells) could be eliminated, since only endothelial, type I and II cells, and macrophages are needed to create a functional alveolar-capillary unit. The correct percentage breakdown of cells is important to assure sufficient paracrine factors and surfactant production.[97-99]

The scaling factor that appears to present the greatest challenge to a μLung is respiration rate. Were we to use allometric scaling, a μLung would have to inspire 643 times per minute to maintain proper oxygenation. Due to the strain this would put on a 1 μm thick polymer membrane, it is likely that this frequency would have to be slowed to prevent rupture. As a result, more surface area would need to be added or higher oxygen concentrations used to compensate for the loss of rate in order to maintain a minute volume of 0.17977 mL/min consumption of oxygen. This highlights the challenges of scaling, especially into the micro- and nano-scales, where the limitations imposed by non-biological fabrication technologies prevent meeting design parameters without violating scaling laws,[100] which could result in a less accurate abstraction. Hence it is critical to specify the desired lung functions and scale the device to achieve them.

Blood

A universal media, or blood surrogate, for HoCs and OoCs must be able to support each cell type in addition to recapitulating the blood's critical role in homeostasis through the transport of dissolved gases, carrier proteins with bound molecules, soluble nutrients, metabolites, and signaling molecules. Since blood "maintenance" is dynamic but tightly controlled by several organs and biochemical processes, development of a blood surrogate is non-trivial.

Allometric scaling of blood components gives some insight into how the surrogate should be constructed. The ESI Scaling Spreadsheet corroborates the scaling issues that must be considered in designing a blood surrogate. First, it can be seen that the concentrations of blood remain virtually the same in organisms of all sizes: conveniently, the concentrations of a remarkably large number of blood components do not scale with body mass.[101] This means that the creation of a blood surrogate can benefit from the large body of work that has been completed on creating cell media. Second, it can be noted that blood volume scales linearly with mass; thus, the total volume of the blood surrogate in an OoC/HoC device should be proportional to the entire size of the device. For all non-aquatic mammals, the blood volume is about 6-7% of the total body volume.[100] Scaling the blood surrogate volume with the size of the OoC/HoC device is necessary to ensure that signaling and other transported molecules are not excessively diluted and that the total mass of transported blood surrogate components is enough to support the organs. Third, the spreadsheet shows the critical functional parameters for ensuring that the cells behave in a physiological manner. The epithelial cells in contact with the blood surrogate must have the same shear stress that cells experience in the body to achieve the requisite polarization. In addition, the cells must experience the same levels of oxygen and carbon dioxide, which are dictated by the gas transport capabilities of the blood surrogate, in order to maintain the physiological metabolism of the cells. The physical properties of a number of different oxygen carriers are also shown. The spreadsheet is based upon the scaling of a complete system; as discussed above, it may be necessary to correct for the hydrodynamic, metabolic, and chemical activity of organs that are not included in the system.

Hence, little should be changed in normal blood to form a blood surrogate. However, there are other scaling issues that must be considered to ensure that the cells in the mHu and μHu behave physiologically.

First, the blood surrogate must recapitulate physiological oxygen transport properties. Experiments have shown that the rate of oxygen delivery to the cells affects the cells' metabolic rate.[102] There are programmatic differences relative to the suitability of serum in an OoC/HoC system: the Defense Threat Reduction Agency (DTRA) program announcement[23] precludes the use of serum, whereas the the Defense Advanced Research Projects Agency (DARPA) program[103] does not. If simple serum-free aqueous culture media is used, the low concentration of dissolved oxygen in the media may limit metabolic rates and affect capillary surface-to-volume scaling. Therefore, the level of oxygen transport that cells experience *in vivo* as enabled by hemoglobin must be functionally mimicked with the blood surrogate. Were erythrocytes not used, perfluorocarbons and hemoglobin-based oxygen carriers may be very effective for achieving this.[104-106] If human or animal serum is not utilized, appropriate concentrations of molecular-carrier proteins such as albumin may be required to replicate organ-organ chemical communication.

For the purpose of supporting HoCs, the blood surrogate must maintain multiple cell types while also optimizing physiological processes. While there is no known universal serum-free media, a number of different formulations of minimal media can be used as a starting point for the creation of a medium that can support multiple cell types.[107;108] To achieve optimal cell functionality and longevity, supplements must be added to this minimal medium.[109]

Although a number of effective medium formulations for the growth and maintenance of multiple cell types have been developed, these media mixtures have not been widely tested for interconnected HoCs. For OoC/HoC systems, this represents a significant challenge due to differential scaling, simultaneous maintenance of multiple cell types, and the recirculatory nature of HoCs. Logic dictates that during flow-through of the blood surrogate within a HoC, some components will be absorbed or metabolized, while others will be added to the blood surrogate, with a negative impact on downstream HoCs.

One method that has been successfully used to create a common blood surrogate for a number of different cells in an OoC/HoC first involves combining the established serum-free mediums of each cell type, which can be found in the literature, to create a base medium. Next, various other components, such as growth factors and supplements, are added to optimize for physiological functionality, based on a number of different physiological measures. Finally, since some of the components of the medium support one type of cell but hinder others, one of several different techniques is used to ensure that each organ receives an optimal subset of the components of the blood surrogate. Zhang *et al*. [108] demonstrated this method by creating a blood surrogate that supported four cultured cell types: liver (C3A), lung (A549), kidney (HK-2), and adipose (HPA). Another option is to grow cells in isolated OoC/HoCs on their preferred media, and then gradually, though controlled valves, wean them slowly from this media to the universal one.

In addition, some properties of blood and related structures that exist physiologically cannot yet be replicated with HoCs. For example, capillaries, which have relatively constant size across species, are too small to be recreated at present, so care must be taken to design the HoCs such that the physical characteristics of the blood surrogate, such as flow, volume, and shear stress, match those found in the tiny capillaries. It is imperative to match the wall shear stress in HoCs to that of microvessels to achieve the same mechanotransduction and gene expression in endothelial cells as in humans.[52] This might be addressed by self-organizing on-chip microvasculature.[66;67]

Furthermore, it is important to understand PK/PD scaling in order to add drugs to the HoC/OoCs at proper levels and to use the HoC/OoCs to predict the pharmacokinetics in humans.[2;3] The classical scaling relationship for drug/signal dosing is that the body's ability to use and metabolize drugs/signals varies with surface area.[110] But these scaling laws are critically dependent on the biochemical mechanisms and physical properties of the organs.[111] If the organs do not functionally mimic physiology, they could fail to predict the PK/PD of humans. Differences in drug transport and metabolism in the HoC can render typical allometric PK/PD scaling useless. This can be seen clearly by the fact that PK/PD varies significantly between infants and adults.[112]

Finally, the blood surrogate will require supporting systems that can provide missing functionality required for blood surrogate and organ maintenance. As required, a microformulator[108] can provide media supplements specific to each organ.[108] The microformulator could be used to locally add media components to a particular organ. A size-exclusion filter or an affinity capture chamber or matrix (Donna Webb, personal communication) could be used to remove any toxic molecules produced by one organ before they reache other organs. Computer-controlled microformulators could also provide the regulated injection of molecules that cannot be maintained by the system alone and those from organs not in the HoC.[24;113]

Cellular Heterogeneity

In contrast to the common monocultures and occasional co-cultures used in much of cellular biology, organs present a much richer cellular heterogeneity. Cellular heterogeneity is a key issue to consider when applying scaling laws to OoCs, since downscaling an organ may result in a reduction in the number of cell types present. Furthermore, achieving a complex co-culture system that preserves native cellular heterogeneity in an organ, much less coupled organs, is still far from realization. As a result, in addition to scaling issues, the choice of cell types used to develop an OoC may also be altered in order to focus on a biological response that is specific to a certain cell population in the organ of interest. Table 2 indicates the relative fractions of the most common cells in each of the organs considered. In the ESI, we present these data in terms of Shannon-Wiener Index (SWI),[114;115] a useful method to quantify cellular heterogeneity. We were unable to identify from the literature a self-consistent set of cell distributions for the kidney. One could also argue that the erythrocytes and leukocytes could be treated separately.

Table 2 Heterogeneity of cell types in different organs.

Organ	# of cell types, *N*	Cell type	%
Brain (Neocortex)[42]	4	Glia	41%
		Neurons	33%
		Vascular	17%
		Microglia	8%
		Total	100%
Heart[59;60]	5	Cardiomyocytes	55%
		Fibroblasts	25%
		Vascular smooth muscle	10%
		Endothelial	7.0%
		Neuronal	3.0%
		Total	100%
Liver[116]	4	Hepatocyte	60%
		Sinusoidal endothelial	20%
		Kupffer	15%
		Hepatic stellate	5.0%
		Total	100%
Lung (Alveolar) [97]	5	Endothelial	39%
		Interstitial	29%
		Type II epithelial	18%
		Type I epithelial	11%
		Alveolar macrophages	3%
		Total	100%
Blood[117]	6	Erythrocytes	99%
		Neutrophils	0.50%
		Lymphocytes	0.30%
		Monocytes	0.050%
		Eosinophils	0.025%
		Basophils	0.007%
		Total	99.9%

Engineering Challenges

We have discussed a number of criteria for scaling mHu and μHu organs as required to design and validate realistic, coupled HoC/OoC systems. That said, there are also a number of engineering challenges that must be met before it is possible to construct a realistic mHu as shown in Fig. 2 or a μHu as shown schematically in Fig. 3. These challenges are cataloged in detail elsewhere,[1] and include determining the proper size of each organ, fluidic control of mL and μL volumes, analytical chemistry in μL and nL volumes, including comprehensive molecular characterization in real time, maintaining and controlling coupled organ systems, vascularizing organs with appropriate surface-to-volume ratios, developing a universal blood surrogate, accounting for missing organs and the adjustment of blood surrogate, modeling coupled organ systems, characterization of organ health and disease, and minimizing

organ cost to enable high-content screening. Several of these can be revisited based upon our detailed scaling analysis.

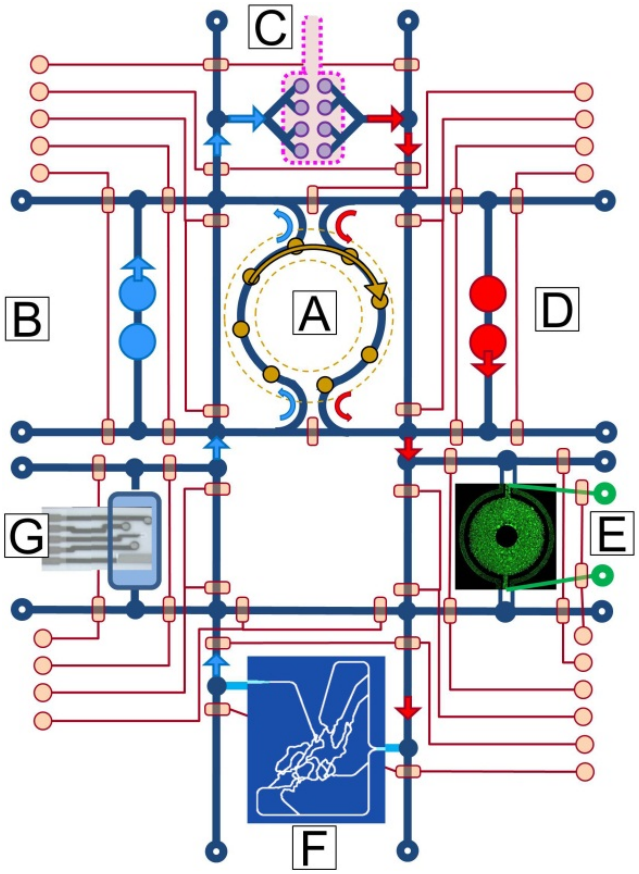

Fig. 3 A concept drawing of a four-organ µHu (*Homo chippiens*). A) An on-chip peristaltic ventricular assist, B) Right heart, C) Lung, D) Left heart, E) Liver (courtesy of Kapil Pant), F) Peripheral circulation[118] (courtesy of Kapil Pant), G) Microchemical analyzer of metabolic activity.[119] The system would operate on a single microfluidic chip, with on-chip pneumatic valves controlling system functions and connections.

The circulating volume of perfusate of an OoC/HoC must match organ size, lest metabolites, hormones, and paracrine signals be diluted to the point that each organ operates in a large reservoir independent of the other organs, thereby precluding accurate study of the desired organ-organ interaction so necessary for PK/PD[120], ADMET,[121] and drug safety/toxicity studies.[122;123] The aforementioned ~4.5 mL and ~4.5µL blood volumes for a mHu and µHu will place severe constraints on not only the fraction of an organ bioreactor that must be occupied by cells, but also limits the size of in-system sensors and the volume that can be withdrawn for analysis of the system's state and subsequent control adjustments. The scaling arguments applied to the organs also apply to the instruments that will analyze their performance.

One might also wonder whether the ratio of cell-to-perfusate volumes alone precludes the use of conventional well plate cell culture in creating properly coupled HoC/OoC systems: blood and interstitial fluid volumes for organs *in vivo* are a small fraction of the volume of the organ itself. Well-plate tissue cultures without internal vascularization can seldom support tissues thicker than 100 to 300 µm without necrosis, so the height of fluid above such tissues grown in a well plate would have to be a small fraction of the thickness of the cell layer to maintain the proper tissue-fluid volume ratios. Because of surface tension effects, it is difficult to pipette fluid from such a thin layer of fluid without damaging the underlying cells. This argues for flow-based HoC/OoC systems that can function within the aforementioned volume constraints. The capabilities of microfluidic systems will be critical to produce compact organs with both appropriate temporal responses and the ability to produce and react to circulating cytokines,[124-126] and to work with small quantities of rare or expensive human cells.[127]

Another issue that has been largely overlooked yet is critical to consider in OoC/HoC design is temporal scaling in reference to disparate cell growth and turnover rates between tissues and between *in vivo* and *in vitro* conditions, particularly when studying drugs with slow kinetics. It is well recognized that cellular co-cultures are subject to being overrun by one of the two cell types, although components can be added to culture media to retard proliferation of one species[128] or accelerate the growth of the other. It may be possible to design a mechanical means to address cellular turnover, for example by adding or removing sections of cells from an organ as the entire MPS ages.

While fluorescence sensors can be used to record metabolic signals such as acidification and oxygenation, it may be wise to reserve optical bandwidth for intracellular fluorescent probes, and instead utilize miniature, wide-bandwidth electrochemical sensors matched to small cell populations[129-131] or single cells.[132-135] It is a great advantage that, typically, the signal-to-noise ratio of electrochemical sensors does not increase as the electrodes are miniaturized,[136] and it has been shown possible to make electrochemical measurements of single cells and small cell populations.[134;135;137;138]

A larger problem is to characterize the circulating molecules either consumed or produced by each organ, given the small volumes and the need to track concentrations of many molecules over long periods of time. Nanospray injection, ion mobility-mass spectrometry (nESI-IM-MS) may prove to be the key technique for rapid OoC state monitoring, given that IM separations require milliseconds rather than the hour or so of high pressure liquid chromatography,[139;140] with the recognition that nESI requires desalting of the media that can now be done on-line.[141] Ultimately, the sensors and controllers might be interconnected in a way that would lead to automated inference of model-based control algorithms.[22;142]

An additional implication of the small fluid volumes in a mHu or µHu is that adjustment of the chemical concentrations of the perfusion media, for example to simulate humeral control of organ function, requires injection of small volumes of precisely mixed fluids. While a high-throughput screening fluidic robot or droplet injector can handle nl to pl volumes, it is a non-trivial to connect one of these into a closed, circulating system of coupled HoCs/OoCs. It is yet another problem to achieve the dynamic range of concentrations of different chemical species found in typical cell culture media without the use of large volumes of media and serial dilution techniques. It will also be necessary to provide the signaling molecules and metabolites from missing organs, as well as apply localized biochemical perturbations to assess the response of the other organs, but note that this has to be done as a small perturbation of the mL to µL volume of the blood surrogate with a temporal resolution guided by the requisite

controller bandwidth. A microfluidic microformulator as we discussed earlier may meet these needs.

As the complexity of a coupled OoC system increases with the number of organs integrated, organ scaling will become more complicated, since the metabolic demands and relative scaling between organs will undoubtedly be affected. We also believe that the scaling in multi-organ OoC/HoC systems, particularly for dynamic metabolic phenomena, will require systematic design such that the functional scaling of any organ system is not significantly altered by another organ, and no single organ receives a substantial, unintended scaling priority.

Coupled non-linear biological systems can spontaneously oscillate and may require external stabilization, which in turn will require the use of sensors and controllers, possibly at the level of each organ. The neurohumoral control of human homeostasis may in fact be simulated by a properly configured sensor and control system, which in turn will benefit from both properly scaled sensors and the ability to rapidly reformulate the perfusion media. That said, regulatory noise may contain useful information about system interconnections.

It will be interesting to determine whether cellular heterogeneity in mixed cultures, critical to cellular signaling mechanisms *in vivo*, can be maintained for long times *in vitro* in coupled HoC/OoC systems. Given the regulatory role of the cellular microenvironment *in vivo*,[143;144] there would be reason to expect that it might in fact become easier to maintain heterogeneity as multiple cell types are grown together in balanced environments with self-conditioned media. The Shannon-Wiener Index may prove important in assessing and controlling this.

We have not yet addressed in detail the scaling issues associated with microfluidics, oxygen carrying capacity of the blood surrogate, and the distributed hydraulic impedance of both the individual organs and the coupled system. This is of particular significance for mHu and μHu systems with working hearts. One would expect that designing around these constraints would benefit greatly from multiphysics, computational biology modeling tools.[145;146] Optimized microfluidic design using a first-principles optimization of vascular branching[147-149] may be better suited than approaches that assume a particular scaling law.[9]

Ultimately, there may be significant technical and economic advantages to creating a μHuman on a single microfluidic chip as shown schematically in Fig. 3. Simpler implementations are already being developed.[108] The total volume of fluidic interconnects is minimized. On-chip valves can be utilized to bypass individual organs while the organs are being seeded and grown to a stable state, and to adjust the duty cycle by which they are connected to the entire system so that conditioning of media can be gradual rather than sudden, providing time for cellular up- and down-regulation of signaling and control genes. Multi-organ integration is not, however, a practical approach until each organ has been perfected individually, albeit at the correct size. Hence as we gain experience in this field, we need to make our HoCs and OoCs small, but not too small.

Conclusions

It is reasonable to assume that the many issues addressed in this review can be resolved through careful attention to engineering and physiological details, particularly with the large number of well-funded investigators now working on this worldwide. Clearly, this does represent a Lab-on-a-Chip challenge of unprecedented complexity and significance. It is most important to recognize that there are obvious trade-offs between realism and simplicity, since the ability to sense and control the microscale environment in microfabricated organs-on-a-chip may provide a solution to the current impasse in extending existing *in vitro* models, most of which are based upon single-layer cellular monoculture, to greater realism and utility.[150]

There will undoubtedly be requests to make these OoC/HoC systems ever-more realistic, and to criticize them for their shortcomings. There have been similar drives for perfect reductionist representations, particularly in the regulatory networks and systems biology communities, where computational models continue to grow in complexity and may operate at a very small rate compared to real time. It is important to realize that OoC/HoC systems reside in a niche of abstraction that will improve constantly with technology but will never exactly recreate a full human, which represents ~10^9 years of evolutionary engineering. It may be most useful if OoCs and HoCs are viewed as simplified model systems for PK/PD and systems biology studies, not small humans.

The drive to perfect reductionism is put in perspective by both Jose Luis Borges and Lewis Carroll, in which a map of an empire/country the size of an empire/country is not found useful.[151;152]Just as a perfect map resolves few problems and produces others, the creation of a near-to-perfect *in vitro* replica of a human may accomplish little at great expense. We believe that with the proper application of scaling and a balance between abstraction and realism, we should be able to learn much about the complexity of human biology[153] and its interaction with drugs from each implementation of a HoC/OoC. Ultimately, we may be able to create OoC/HoC surrogates for specific genetic or disease subgroups for drug development or for individual patients to optimize their treatment.

Notes and references

† Electronic Supplementary Information (ESI) available: Discussion of the Shannon-Wiener Index, and a Scaling Spreadsheet that provides an extensive table describing scaling parameters for brain, heart, kidney, liver, lung, and blood. See DOI: 10.1039/b000000x/

Acknowledgements

We thank Rashi Iyer and Kapil Pant for their contributions to Figs. 2 and 3, and Allison Price and Don Berry for their editorial assistance. We have benefitted from extensive discussions with Frank E. Block, Jr., Frank E. Block III, David Cliffel, William Fissell, Geraldine Hamilton, Donald Ingber, Rashi Iyer, Daniel Levner, John McLean, Kapil Pant, Kevin Kit Parker, Andrzej Przekwas, and Philip Samson regarding microfluidic devices and organs-on-a-chip. This research has been funded in part by Defense Threat Reduction Agency grants HDTRA1-09-1-00-13 and DTRA100271A-5196; NIH grants R01GM092218, RC2DA028981, and, through the NIH Common Fund, NCATS grant 1UH2-TR000491-01; DARPA grant W911NF-12-2-0036; the NSF Graduate Research Fellow Program (BCE); and the Vanderbilt Institute for Integrative Biosystems Research and Education (VIIBRE) and a Vanderbilt University Discovery

Grant. The content is solely the responsibility of the authors and does not necessarily represent the official views of the funding agencies and institutions.

References

1. J. P. Wikswo, F. E. Block III, D. E. Cliffel, C. R. Goodwin, C. C. Marasco, D. A. Markov, D. L. McLean, J. A. McLean, J. R. McKenzie, R. S. Reiserer, P. C. Samson, D. K. Schaffer, K. T. Seale, and S. D. Sherrod, *IEEE Trans.Biomed.Eng.*, 2013**, 60**, 682.
2. M. B. Esch, T. L. King, and M. L. Shuler, *Annu.Rev.Biomed.Engr.*, 2011**, 13**, 55.
3. M. Shuler, *Ann.Biomed.Eng.*, 2012**, 40**, 1399.
4. K. Schmidt-Nielsen, *J.Exp.Zool.*, 1975**, 194**, 287.
5. M. Kleiber, *Hilgardia*, 1932**, 6**, 315.
6. M. Kleiber, *Proceedings of the Society for Experimental Biology and Medicine.Society for Experimental Biology and Medicine (New York, N.Y.)*, 1941**, 48**, 419.
7. K. Schmidt-Nielsen, in *Scaling: Why is animal size so important?*, Cambridge University Press, New York, 1984, ch. Chapter 8, pp. 90-98.
8. P. S. Dodds, D. H. Rothman, and J. S. Weitz, *J.Theor.Biol.*, 2001**, 209**, 9.
9. G. B. West, J. H. Brown, and B. J. Enquist, *Science*, 1997**, 276**, 122.
10. J. H. Brown, V. K. Gupta, B. L. Li, B. T. Milne, C. Restrepo, and G. B. West, *Philos.T.Roy.Soc.London B*, 2002**, 357**, 619.
11. S. L. Lindstedt and W. A. Calder, *Quart.Rev.Biol.*, 1981**, 56**, 1.
12. W. R. Stahl, *Science*, 1965**, 150**, 1039.
13. T. N. Johnson, A. Rostami-Hodjegan, and G. T. Tucker, *Clin.Pharmacokinet.*, 2006**, 45**, 931.
14. M. Danhof, J. de Jongh, E. C. M. De Lange, O. Della Pasqua, B. A. Ploeger, and R. A. Voskuyl, *Annu.Rev.Pharmacol.Toxicol.*, 2007**, 47**, 357.
15. H. W. Leung, in *General, Applied and Systems Toxicology*, John Wiley & Sons, Ltd, 2009.
16. M. Hadi, I. M. Westra, V. Starokozhko, S. Dragovic, M. T. Merema, and G. M. M. Groothuis, *Chem.Res.Toxicol.*, 2013**, doi:10.1021/tx300519p**.
17. D. Huh, D. C. Leslie, B. D. Matthews, J. P. Fraser, S. Jurek, G. A. Hamilton, K. S. Thorneloe, M. A. Mcalexander, and D. E. Ingber, *Sci.Transl.Med.*, 2012**, 4**, 159ra147.
18. D. Huh, B. D. Matthews, A. Mammoto, M. Montoya-Zavala, H. Y. Hsin, and D. E. Ingber, *Science*, 2010**, 328**, 1662.
19. A. Grosberg, P. W. Alford, M. L. McCain, and K. K. Parker, *Lab Chip*, 2011**, 11**, 4165.
20. P. W. Alford, A. W. Feinberg, S. P. Sheehy, and K. K. Parker, *Biomaterials*, 2010**, 31**, 3613.
21. H. J. Kim, D. Huh, G. Hamilton, and D. E. Ingber, *Lab Chip*, 2012**, 12**, 2165.
22. P. R. LeDuc, W. C. Messner, and J. P. Wikswo, *Annu.Rev.Biomed.Engr.*, 2011**, 13**, 369.
23. Chemical and Biological Defense Innovations and Technologies, Grants.gov, 12 Dec. 2011. http://www.grants.gov/search/search.do?mode=VIEW&oppId=133833
24. C. L. Hansen, M. O. A. Sommer, and S. R. Quake, *PNAS (US)*, 2004**, 101**, 14431.
25. C. L. Hansen, Caltech, 2004.
26. R. Yang, M. Zhang, and T. J. Tarn, in *Life science automation fundamentals and applications*, ed.M. Zhang, B. Nelson, R. Felder, Artech House, Norwood, MA, 2007, ch. Chapter 6, pp. 153-196.
27. L. Cucullo, N. Marchi, M. Hossain, and D. Janigro, *J.Cereb.Blood Flow Metab.*, 2011**, 31**, 767.
28. R. Booth and H. Kim, *Lab Chip*, 2012**, 12**, 1784.
29. A. K. H. Achyuta, A. J. Conway, R. B. Crouse, E. C. Bannister, R. N. Lee, C. P. Katnik, A. A. Behensky, J. Cuevas, and S. S. Sundaram, *Lab Chip*, 2013**, 13**, 542.
30. L. M. Griep, F. Wolbers, B. de Wagenaar, P. M. ter Braak, B. B. Weksler, I. A. Romero, P. O. Couraud, I. Vermes, A. D. van der Meer, and A. van den Berg, *Biomed.Microdevices*, 2013**, 15**, 145.
31. B. Prabhakarpandian, M. C. Shen, J. B. Nichols, I. R. Mills, M. Sidoryk-Wegrzynowicz, M. Aschner, and K. Pant, *Lab Chip*, 2013**, 13**, 1093.
32. Y. Gao, D. Majumdar, B. Jovanovic, C. Shaifer, P. Lin, A. Zijlstra, D. Webb, and D. Li, *Biomed.Microdevices*, 2011**, 13**, 539.
33. D. Majumdar, Y. Gao, D. Li, and D. J. Webb, *J.Neurosci.Methods*, 2011**, 196**, 38.
34. J. Park, H. Koito, J. Li, and A. Han, *Lab Chip*, 2012**, DOI: 10.1039/C2LC40303J**.
35. M. Shi, D. Majumdar, Y. Gao, B. M. Brewer, C. R. Goodwin, J. A. McLean, D. Li, and D. J. Webb, *Lab Chip*, 2013**, Advance article. doi: 10.1039/C3LC50249J** .
36. S. Herculano-Houzel, P. Ribeiro, L. Campos, A. V. da Silva, L. B. Torres, K. C. Catania, and J. H. Kaas, *Brain Behav.Evol.*, 2011**, 78**, 302.
37. K. Chung, J. Wallace, S. Y. Kim, S. Kalyanasundaram, A. S. Andalman, T. J. Davidson, J. J. Mirzabekov, K. A. Zalocusky, J. Mattis, A. K. Denisin, S. Pak, H. Bernstein, C. Ramakrishnan, L. Grosenick, V. Gradinaru, and K. Deisseroth, *Nature*, 2013**, advance online publication, doi:10.1038/nature12107**.
38. S. Herculano-Houzel, *Front.Hum.Neurosci.*, 2009**, 3**, Article 31.
39. B. Davies and T. Morris, *Pharm.Res.*, 1993**, 10**, 1093.
40. S. Herculano-Houzel, *PloS.One.*, 2011**, 6**, Article e17514.
41. J. Karbowski, *BMC Biol.*, 2007**, 5**, Article 18.
42. L. Lyck, I. D. Santamaria, B. Pakkenberg, J. Chemnitz, H. D. Schroder, B. Finsen, and H. J. G. Gundersen, *J.Neurosci.Methods*, 2009**, 182**, 143.
43. P. Kreczmanski, H. Heinsen, V. Mantua, F. Woltersdorf, T. Masson, N. Ulfig, R. Schmidt-Kastner, H. Korr, H. W. M. Steinbusch, P. R. Hof, and C. Schmitz, *Acta Neuropathol.(Berl).*, 2009**, 117**, 409.
44. A. Armulik, G. Genove, and C. Betsholtz, *Dev.Cell*, 2011**, 21**, 193.
45. T. M. Mathiisen, K. P. Lehre, N. C. Danbolt, and O. P. Ottersen, *Glia*, 2010**, 58**, 1094.
46. D. E. Sims, *Tissue Cell*, 1986**, 18**, 153.

47. H. Ito, I. Kanno, C. Kato, T. Sasaki, K. Ishii, Y. Ouchi, A. Iida, H. Okazawa, K. Hayashida, N. Tsuyuguchi, K. Ishii, Y. Kuwabara, and M. Senda, *European Journal of Nuclear Medicine and Molecular Imaging*, 2004**, 31**, 635.
48. L. C. Mchenry, *N.Engl.J.Med.*, 1966**, 274**, 82.
49. L. C. Mchenry, *N.Engl.J.Med.*, 1965**, 273**, 562.
50. P. Lebrungrandie, J. C. Baron, F. Soussaline, C. Lochh, J. Sastre, and M. G. Bousser, *Arch.Neurol.*, 1983**, 40**, 230.
51. L. Cucullo, M. Hossain, V. Puvenna, N. Marchi, and D. Janigro, *BMC Neurosci.*, 2011**, 12**, 40.
52. A. G. Koutsiaris, S. V. Tachmitzi, N. Batis, M. G. Kotoula, C. H. Karabatsas, E. Tsironi, and D. Z. Chatzoulis, *Biorheology*, 2007**, 44**, 375.
53. J. M. Tarbell, *Cardiovasc.Res.*, 2010**, 87**, 320.
54. Y. Tanaka, K. Morishima, T. Shimizu, A. Kikuchi, M. Yamato, T. Okano, and T. Kitamori, *Lab Chip*, 2006**, 6**, 362.
55. J. Park, I. C. Kim, J. Baek, M. Cha, J. Kim, S. Park, J. Lee, and B. Kim, *Lab Chip*, 2007**, 7**, 1367.
56. J. C. Nawroth, H. Lee, A. W. Feinberg, C. M. Ripplinger, M. L. McCain, A. Grosberg, J. O. Dabiri, and K. K. Parker, *Nat.Biotechnol.*, 2012**, 30**, 792.
57. E. J. Lee, D. E. Kim, E. U. Azeloglu, and K. D. Costa, *Tissue Eng.Pt.A*, 2008**, 14**, 215.
58. G. A. Giridharan, M. D. Nguyen, R. Estrada, V. Parichehreh, T. Hamid, M. A. Ismahil, S. D. Prabhu, and P. Sethu, *Anal.Chem.*, 2010**, 82**, 7581.
59. I. Banerjee, J. W. Fuseler, R. L. Price, T. K. Borg, and T. A. Baudino, *Am.J.Physiol.Heart*, 2007**, 293**, H1883.
60. D. L. Brutsaert, *Physiol.Rev.*, 2003**, 83**, 59.
61. M. Horackova and J. A. Armour, *Cardiovasc.Res.*, 1995**, 30**, 326.
62. M. Horackova and Z. Byczko, *Exp.Cell Res.*, 1997**, 237**, 158.
63. M. Horackova, M. H. Huang, J. A. Armour, D. A. Hopkins, and C. Mapplebeck, *Cardiovasc.Res.*, 1993**, 27**, 1101.
64. K. Lemmens, V. F. M. Segers, M. Demolder, and G. W. De Keulenaer, *J.Biol.Chem.*, 2006**, 281**, 19469.
65. T. M. Leucker, M. Bienengraeber, M. Muravyeva, I. Baotic, D. Weihrauch, A. K. Brzezinska, D. C. Warltier, J. R. Kersten, and P. F. Pratt, *J.Mol.Cell.Cardiol.*, 2011**, 51**, 803.
66. Y. H. Hsu, M. L. Moya, P. Abiri, C. C. W. Hughes, S. C. George, and A. P. Lee, *Lab Chip*, 2013**, 13**, 81.
67. M. L. Moya, Y.-H. Hsu, A. P. Lee, C. C. W. Hughes, and S. C. George, *Tissue Eng.Pt.C:* 2013**, In press**.
68. T. G. Papaioannou, E. N. Karatzis, M. Vavuranakis, J. P. Lekakis, and C. Stefanadis, *Int.J.Cardiol.*, 2006**, 113**, 12.
69. W. H. Fissell, J. Kimball, S. M. Mackay, A. Funke, and H. D. Humes, *Ann.New York Acad.Sci.*, 2001**, 944**, 284.
70. H. D. Humes, S. M. Mackay, A. J. Funke, and D. A. Buffington, *Kidney Int.*, 1999**, 55**, 2502.
71. E. M. Wright, *Am.J.Physiol.Renal*, 2001**, 280**, F10.
72. S. Abrahams, L. Greenwald, and D. L. Stetson, *Am.J.Physiol.*, 1991**, 261**, R719.
73. C. A. Beuchat, *J.Theor.Biol.*, 1990**, 143**, 113.
74. R. Greger, *Physiol.Rev.*, 1985**, 65**, 760.
75. S. Kurbel, K. Dodig, and R. Radic, *Adv.Physiol.Educ.*, 2002**, 26**, 278.
76. C. A. Beuchat, *Am.J.Physiol-Reg.I.*, 1996**, 271**, R157.
77. J. W. Prothero, *Comparative Biochemistry and Physiology Part A: Physiology*, 1982**, 71**, 567.
78. Y. Nahmias, F. Berthiaume, and M. L. Yarmush, *Adv.Biochem.Eng.Biotechnol.*, 2007**, 103**, 309.
79. A. K. Sohlenius-Sternbeck, *Toxicol.in Vitro*, 2006**, 20**, 1582.
80. B. D. Foy, A. Rotem, M. Toner, R. G. Tompkins, and M. L. Yarmush, *Cell.Transplant.*, 1994**, 3**, 515.
81. U. J. Balis, K. Behnia, B. Dwarakanath, S. N. Bhatia, S. J. Sullivan, M. L. Yarmush, and M. Toner, *Metab.Eng.*, 1999**, 1**, 49.
82. S. C. Balmert, D. McKeel, F. Triolo, B. Gridelli, K. Zeilinger, R. Bornemann, and J. C. Gerlach, *Int.J.Artif.Organs*, 2011**, 34**, 410.
83. K. Zeilinger, T. Schreiter, M. Darnell, T. Soderdahl, M. Lubberstedt, B. Dillner, D. Knobeloch, A. K. Nussler, J. C. Gerlach, and T. B. Andersson, *Tissue Eng.Pt.C:* 2011**, 17**, 549.
84. J. M. Piret and C. L. Cooney, *Biotechnol.Bioeng.*, 1991**, 37**, 80.
85. W. G. Whitford and J. J. S. Cadwell, *BioProcess Int.*, 2009**, 7**, 54.
86. I. Mahmood, *J.Pharm.Sci.*, 2005**, 94**, 883.
87. T. Lave, S. Dupin, C. Schmitt, R. C. Chou, D. Jaeck, and P. Coassolo, *J.Pharm.Sci.*, 1997**, 86**, 584.
88. Y. Naritomi, S. Terashita, A. Kagayama, and Y. Sugiyama, *Drug Metab.Dispos.*, 2003**, 31**, 580.
89. Y. Naritomi, S. Terashita, S. Kimura, A. Suzuki, A. Kagayama, and Y. Sugiyama, *Drug Metab.Dispos.*, 2001**, 29**, 1316.
90. H. Boxenbaum, *J.Pharmacokinet.Biopharm.*, 1980**, 8**, 165.
91. D. J. Carlile, K. Zomorodi, and J. B. Houston, *Drug Metab.Dispos.*, 1997**, 25**, 903.
92. G. Ghibellini, L. S. Vasist, E. M. Leslie, W. D. Heizer, R. J. Kowalsky, B. F. Calvo, and K. L. R. Brouwer, *Clin.Pharmacol.Ther.*, 2007**, 81**, 406.
93. R. J. Riley, D. F. McGinnity, and R. P. Austin, *Drug Metab.Dispos.*, 2005**, 33**, 1304.
94. J. S. Miller, K. R. Stevens, M. T. Yang, B. M. Baker, D. H. Nguyen, D. M. Cohen, E. Toro, A. A. Chen, P. A. Galie, X. Yu, R. Chaturvedi, S. N. Bhatia, and C. S. Chen, *Nat.Mater.*, 2012**, 11**, 768.
95. E. R. Weibel, *Annu.Rev.Physiol.*, 1987**, 49**, 147.
96. C. Hou and M. Mayo, *Phys.Rev.E*, 2011**, 84**, Article 061915.
97. J. D. Crapo, B. E. Barry, P. Gehr, M. Bachofen, and E. R. Weibel, *Am.Rev.Respir.Dis.*, 1982**, 126**, 332.
98. W. A. H. Wallace, M. Gillooly, and D. Lamb, *Thorax*, 1992**, 47**, 437.
99. A. O. S. Fels and Z. A. Cohn, *J.Appl.Physiol.*, 1986**, 60**, 353.
100. W. R. Stahl, *J.Appl.Physiol.*, 1967**, 22**, 453.
101. M. Kjeld and O. Olafsson, *Can.J.Zool.*, 2008**, 86**, 890.
102. M. F. Brown, T. P. Gratton, and J. A. Stuart, *Am.J.Physiol-Reg.I.*, 2007**, 292**, R2115.
103. Microphysiological Systems, Solicitation no. DARPA-BAA-11-73 FedBizOpps.gov, 11 Sept. 2011. https://www.fbo.gov/index?s=opportunity&mode=form&id=956b160c42aaa386cf5762f12c21be9f&tab=core&_cview=0
104. G. Chen and A. F. Palmer, *Biotechnol.Progr.*, 2009**, 25**, 1317.
105. D. R. Spahn, *Critical Care*, 1999**, 3**, R93.
106. M. Yamazaki, R. Aeba, R. Yozu, and K. Kobayashi, *Circulation*, 2006**, 114, suppl 1**, I220.

107. V. Jager, J. Lehmann, and P. Friedl, *Cytotechnology*, 1988**, 1**, 319.
108. C. Zhang, Z. Q. Zhao, N. A. A. Rahim, D. van Noort, and H. Yu, *Lab Chip*, 2009**, 9**, 3185.
109. J. van der Valk, D. Brunner, K. De Smet, A. F. Svenningsen, P. Honegger, L. E. Knudsen, T. Lindl, J. Noraberg, A. Price, M. L. Scarino, and G. Gstraunthaler, *Toxicol.in Vitro*, 2010**, 24**, 1053.
110. D. Pinkel, *Cancer Res.*, 1958**, 18**, 853.
111. C. Hall, E. Lueshen, A. Mosat, and A. A. Linninger, *J.Pharm.Sci.*, 2012**, 101**, 1221.
112. V. Sharma and J. H. McNeill, *Br.J.Pharmacol.*, 2009**, 157**, 907.
113. A. H. Diercks, A. Ozinsky, C. L. Hansen, J. M. Spotts, D. J. Rodriguez, and A. Aderem, *Anal.Biochem.*, 2009**, 386**, 30.
114. L. Jost, *Oikos*, 2006**, 113**, 363.
115. C. J. Keylock, *Oikos*, 2005**, 109**, 203.
116. D. E. Malarkey, K. Johnson, L. Ryan, G. Boorman, and R. R. Maronpot, *Toxicologic Pathology*, 2005**, 33**, 27.
117. L. Sherwood, in *Human physiology: from cells to systems*, Cengage-Brooks/Cole, Belmont, CA, 7th ed., 2010.
118. B. Prabhakarpandian, Y. Wang, A. Rea-Ramsey, S. Sundaram, M. F. Kiani, and K. Pant, *Microcirculation*, 2011**, 18**, 380.
119. L. A. Hiatt, J. R. McKenzie, L. F. Deravi, R. S. Harry, D. W. Wright, and D. E. Cliffel, *Biosens.Bioelectron.*, 2012**, 33**, 128.
120. J. H. Sung, C. Kam, and M. L. Shuler, *Lab Chip*, 2010**, 10**, 446.
121. K. Viravaidya and M. L. Shuler, *Biotechnol.Progr.*, 2004**, 20**, 590.
122. F. D. Sistare and J. J. DeGeorge, *Biomarkers Med.*, 2011**, 5**, 497.
123. B. Ma, G. Zhang, J. Qin, and B. Lin, *Lab Chip*, 2009**, 9**, 232.
124. J. P. Wikswo, A. Prokop, F. Baudenbacher, D. Cliffel, B. Csukas, and M. Velkovsky, *IEE Proc.-Nanobiotechnol.*, 2006**, 153**, 81.
125. A. Prokop, Z. Prokop, D. Schaffer, E. Kozlov, J. P. Wikswo, D. Cliffel, and F. Baudenbacher, *Biomed.Microdevices*, 2004**, 6**, 325.
126. S. Faley, K. Seale, J. Hughey, D. K. Schaffer, S. VanCompernolle, B. McKinney, F. Baudenbacher, D. Unutmaz, and J. P. Wikswo, *Lab Chip*, 2008**, 8**, 1700.
127. S. L. Faley, M. Copland, D. Wlodkowic, W. Kolch, K. T. Seale, J. P. Wikswo, and J. M. Cooper, *Lab Chip*, 2009**, 9**, 2659.
128. A. Suzumura, S. Bhat, P. A. Eccleston, R. P. Lisak, and D. H. Silberberg, *Brain Res.*, 1984**, 324**, 379.
129. S. E. Eklund, D. E. Cliffel, E. Kozlov, A. Prokop, J. P. Wikswo, Jr., and F. J. Baudenbacher, *Anal.Chim.Acta*, 2003**, 496**, 93.
130. S. E. Eklund, R. M. Snider, J. Wikswo, F. Baudenbacher, A. Prokop, and D. E. Cliffel, *J.Electroanal.Chem.*, 2006**, 587**, 333.
131. S. E. Eklund, R. G. Thompson, R. M. Snider, C. K. Carney, D. W. Wright, J. Wikswo, and D. E. Cliffel, *Sensors*, 2009**, 9**, 2117.
132. I. A. Ges and F. Baudenbacher, *Biosens.Bioelectron.*, 2010**, 26**, 828.
133. I. A. Ges and F. Baudenbacher, *Biosens.Bioelectron.*, 2010**, 25**, 1019.
134. I. A. Ges, I. A. Dzhura, and F. J. Baudenbacher, *Biomed.Microdevices*, 2008**, 10**, 347.
135. I. A. Ges and F. Baudenbacher, *J.Exp.Nanosci.*, 2008**, 3**, 63.
136. D. Grieshaber, R. MacKenzie, J. Voeroes, and E. Reimhult, *Sensors*, 2008**, 8**, 1400.
137. M. Ciobanu, D. E. Taylor, J. P. Wilburn, and D. E. Cliffel, *Anal.Chem.*, 2008**, 80**, 2717.
138. I. A. Ges and F. J. Baudenbacher, *Biosens.Bioelectron.*, 2008.
139. J. R. Enders, C. C. Marasco, A. Kole, B. Nguyen, S. Sundarapandian, K. T. Seale, J. P. Wikswo, and J. A. Mclean, *IET Syst.Biol.*, 2010**, 4**, 416.
140. J. R. Enders, C. R. Goodwin, C. C. Marasco, K. T. Seale, J. P. Wikswo, and J. A. Mclean, *Spectroscopy Supp.Curr.Trends Mass Spectrometry*, 2011**, July**, 18.
141. J. R. Enders, C. C. Marasco, J. P. Wikswo, and J. A. Mclean, *Anal.Chem.*, 2012**, 84**, 8467.
142. M. D. Schmidt, R. R. Vallabhajosyula, J. W. Jenkins, J. E. Hood, A. S. Soni, J. P. Wikswo, and H. Lipson, *Phys.Biol.*, 2011**, 8**, 055011.
143. L. G. Griffith and M. A. Swartz, *Nature Rev.Mol.Cell Biol.*, 2006**, 7**, 211.
144. D. E. Ingber, *Semin.Cancer.Biol.*, 2008**, 18**, 356.
145. R. Kannan and A. Przekwas, *Int.J.Numer.Meth.Biomed.Eng.*, 2011**, 27**, 13.
146. A. J. Przekwas, M. R. Somayaji, and Z. J. Chen, *CoBi Tools for model Guided Manufacturing of Biologics from Synthetically Stimulated Biofactories*, 2011.
147. A. Bejan and S. Lorente, *Physics of Life Reviews*, 2011**, 8**, 209.
148. S. Lorente, W. Wechsatol, and A. Bejan, *Int.J.Heat Mass Tran.*, 2002**, 45**, 3299.
149. W. Wechsatol, S. Lorente, and A. Bejan, *Int.J.Heat Mass Tran.*, 2002**, 45**, 4911.
150. A. D. van der Meer and A. van den Berg, *Integr.Biol.*, 2012**, 4**, 461.
151. J. L. Borges and N. T. tr- Di Giovanni, in *A Universal History of Infamy*, Penguin, London, 1975.
152. L. Carroll, in *The complete Sylvie and Bruno*, Mercury House, San Francisco, 1991, ch. Chapter 11, pp. 262-267.
153. S. Huang and J. Wikswo, in *Reviews of Physiology, Biochemistry and Pharmacology*, ed.S. G. Amara, E. Bamberg, T. Gudermann, S. C. Hebert, R. Jahn, W. J. Lederer, R. Lill, A. Miyajima, S. Offermanns, 157 edn., 2007, vol. 157, pp. 81-104.

Scaling and systems biology for integrating multiple organs-on-a-chip

John P. Wikswo* [a,b,c], Erica L. Curtis,[a,b] Zachary E. Eagleton,[a,b] Brian C. Evans,[a,b] Ayeeshik Kole,[a,b] Lucas H. Hofmeister,[a,b] and William J. Matloff[a,b]

Electronic Supplementary Information (ESI)

We provide in both PDF and Excel formats a Scaling Spreadsheet with ~250 physiological parameters describing brain, heart, kidney, liver, lung, and blood. In this section, we also discuss in more detail than in the manuscript the Shannon-Wiener Index as a measure of cellular heterogeneity.

Cellular Heterogeneity

The Shannon-Wiener Index (*SWI*)[1;2] provides a useful measure of the effective heterogeneity of organs that can guide organ-on-chip (OoC) and human organ construct (HOC) design:

$$SWI = -\sum_{i}^{N} p_i \log_2 p_i \ ,$$

where there are N cell types and p_i is the probability that a cell is of type i. By using log base 2, we compute *SWI* in bits. The Diversity Index (*DI*)[1] is simply 2^{SWI} and indicates the effective number of cell types in the tissue. If we have only one cell type in a tissue, then $SWI = -1 \log_2 1 = 0$, and $DI = 1$. If we have two cell types that are equally abundant (*i.e.*, $p_1 = p_2 = 0.5$), $SWI = -(0.5 \log_2(0.5) + 0.5 \log_2(0.5)) = -(0.5 \times -1 + 0.5 \times -1) = 1$. If we have two cell types with disparate abundances (*e.g.*, $p_1 = 0.1$ and $p_2 = 0.9$), then $SWI = -(0.1 \log_2(0.1) + 0.9 \log_2(0.9)) = -(0.1 \times -3.32 + 0.9 \times -.152) = -(-.332 + -.136) = 0.469$, and $DI = 2^{0.469} = 1.38$. So the more monodisperse (less heterogeneous) is a two-cell tissue, the closer the *SWI* is to 0 because one cell type dominates. The more heterogeneous the tissue, then the closer is *SWI* to 1, since each cell type is equally represented ($DI = 2$). If the abundance of the two cell types is imbalanced, then the SI is intermediate between 1 and 2. Table S1 lists *SWI* and *DI* for several organs, which we can use in designing and validating OoCs and HoCs. The sources of the brain data are listed in the Scaling Spreadsheet. We were unable to identify from the literature a self-consistent set of cell distributions for the kidney.

Table S1 Heterogeneity of cell types in different organs and the corresponding the Shannon-Wiener Index (*SWI*), in bits, and the effective number of cell types, known as the diversity index ($DI = 2^{SWI}$)

Organ	# of cell types, *N*	Cell type	%	Shannon-Wiener Index, *SWI*	Diversity Index, *DI*	$P_i = 1/N$ for uniform distribution of *N* cell types	*SWI* for uniform cell-type distribution
Brain (Neocortex)[3]	4	Glia	41%				
		Neurons	33%				
		Vascular	17%				
		Microglia	8%				
		Total	100%	1.8	3.4	0.25	2.0
Heart[4;5]	5	Cardiomyocytes	55%				
		Fibroblasts	25%				
		Vascular smooth muscle	10%				
		Endothelial	7%				
		Neuronal	3%				
		Total	100%	1.7	3.3	0.20	2.3
Liver[6]	4	Hepatocyte	60%				
		Sinusoidal endothelial	20%				
		Kupffer	15%				
		Hepatic stellate	5%				
		Total	100%	1.5	2.9	0.25	2.0
Lung (Alveolar)[7]	5	Endothelial	39%				
		Interstitial	29%				
		Type II epithelial	18%				
		Type I epithelial	11%				
		Alveolar macrophages	3%				
		Total	100%	2.0	4.0	0.20	2.3
Blood[8]	6	Erythrocytes	99%				
		Neutrophils	0.50%				
		Lymphocytes	0.30%				
		Monocytes	0.050%				
		Eosinophils	0.025%				
		Basophils	0.007%				
		Total	99.9%	0.1	0.1	0.20	2.3

a Vanderbilt Institute for Integrative Biosystems Research and Education, Nashville, TN 37235, USA. E-mail: john.wikswo@vanderbilt.edu
b Department of Biomedical Engineering, Vanderbilt University, Nashville, TN 37235, USA
c Department of Molecular Physiology & Biophysics and Department of Physics & Astronomy, Vanderbilt University, Nashville, TN 37235, USA

Scaling Spreadsheet

The following pages contain a PDF of **Table S1. Structural and functional parameters to guide the scaling of organs-on-chips and human organ constructs based upon human and animal data.** This is in the form of a spread sheet, with ~250 parameters from brain, heart, kidney, liver, lung and blood that are useful in designing coupled organs on a chip. The user is urged to validate all numbers from the primary references therein and report any discrepancies to the authors. A live version of the spread sheet can be downloaded from http://www.vanderbilt.edu/viibre/organs-on-a-chip.php . There is a moderated section for comments on and additions to the table.

References

1. **L. Jost, *Oikos*, 2006, 113, 363.**
2. **C. J. Keylock, *Oikos*, 2005, 109, 203.**
3. **L. Lyck, I. D. Santamaria, B. Pakkenberg, J. Chemnitz, H. D. Schroder, B. Finsen, and H. J. G. Gundersen, *J.Neurosci.Methods*, 2009, 182, 143.**
4. **I. Banerjee, J. W. Fuseler, R. L. Price, T. K. Borg, and T. A. Baudino, *Am.J.Physiol.Heart*, 2007, 293, H1883.**
5. **D. L. Brutsaert, *Physiol.Rev.*, 2003, 83, 59.**
6. **D. E. Malarkey, K. Johnson, L. Ryan, G. Boorman, and R. R. Maronpot, *Toxicologic Pathology*, 2005, 33, 27.**
7. **K. C. Stone, R. R. Mercer, P. Gehr, B. Stockstill, and J. D. Crapo, *Am.J.Respir.Cell Mol.Biol.*, 1992, 6, 235.**
8. **L. Sherwood, in *Human physiology: from cells to systems*, Cengage-Brooks/Cole, Belmont, CA, 7th ed., 2010.**

Table S1. Structural and functional parameters to guide the scaling of organs-on-chips and human organ constructs based upon human and animal data. The user is urged to validate all numbers from the primary references cited and report any discrepancies to john.wikswo@vanderbilt.edu
Version: 6/10/2013
A live version of the spread sheet can be downloaded from http://www.vanderbilt.edu/viibre/organs-on-a-chip.php . There is a moderated section for comments on and additions to the table.

									Hu mass, kg	7.00E+01	mHu mass, kg	7.00E-02	Mouse mass, kg	2.00E-02	uH mass, kg	7.00E-05	nH mass, kg	7.00E-08	<<ENTER MASS	
Organ	Type of Quantity	Quantity	Base unit	Allometric coefficient A	Allometric power B	+/-	SE	Allometric Reference Unit	Notes	Human (Hu)	± SE	mHu Allometric	mHu Functional	Mouse	± SE	uH Allometric	uH Functional	nH Allometric	nH Functional	References
Brain																				
Brain	Structural	Organ volume	L	0.029	0.922				Scaled to body mass. Brain Mass and volume scale linearally	1.45E+00		2.50E-03	1.45E-03			4.28E-06	1.45E-06	7.34E-09	1.45E-09	1
Brain	Structural	Intracranial Volume	mm^3						Total volume of gray matter+White matter+cerebrospinal fluid	1.50E+06	0.15	N/A	1.50E+03			N/A	1.50E+00	N/A	1.50E-03	2
Brain	Structural	Gray Matter V	cm^3						gray matter mass=volume (cm^3)	5.72E+02		N/A	5.72E-01			N/A	5.72E-04	N/A	5.72E-07	
Brain	Structural	White Matter V	cm^3	1	1.23				Scaled to gray matter volume	2.46E+03		N/A	2.46E+00			N/A	2.46E-03	N/A	2.46E-06	3
Brain	Structural	White Matter V	cm^2	1	1.243	+/-	0.036		White matter surface area is used to derive White Matter Volume	2.69E+03		N/A	2.69E+00			N/A	2.69E-03	N/A	2.69E-06	3
Brain	Structural	Interstitial Volume	uL						Extracellular space is 200ul/g tissue LHH ref 28	3.02E+05		N/A	3.02E+02			N/A	3.02E-01	N/A	3.02E-04	4
Brain	Structural	Organ Mass (primates)	g	0.029	0.922				Scaled to body mass	1.51E+03	299.14	2.50E+00	1.51E+00	4.16E-01		4.28E-03	1.51E-03	7.34E-06	1.51E-06	1;5
Brain	Structural	Cerebellum Mass	g							1.54E+02	19.29	N/A	1.54E-01	5.60E-02		N/A	1.54E-04	N/A	1.54E-07	5
Brain	Structural	Rest of Brain Mass	g							1.18E+02	45.42	N/A	1.18E-01			N/A	1.18E-04	N/A	1.18E-07	5
Brain	Structural	Whole Cortical Mass	g	1.05E-08	1.097	+/-	0.081		Scaled to # gray matter neurons. Mass from LHH Ref 2.	1.23E+03	233.68	N/A	6.31E-01	1.73E-01		N/A	3.23E-04	N/A	1.65E-07	3;5
Brain	Structural	Cortical White Matter Mass	g	4.35E-10	1.197	+/-	0.091		Scaled to # gray matter neurons. >40% of cerebral cortex in humans, mass of one hemisphere from LHH Ref 2.	5.23E+02	119.7	N/A	1.34E-01			N/A	3.44E-05	N/A	8.81E-09	3
Brain	Structural	Cortical White Matter Mass	g	3.88E-09	1.032	+/-	0.04		Scaled to # of cortical non-neuronal cells. Other cells are primarily oligodendrocytes	5.23E+02	119.7	N/A	4.19E-01			N/A	3.36E-04	N/A	2.69E-07	3
Brain	Structural	Cortical White Matter Mass	g	0.3572094	1.148				Scaled to gray matter mass	5.23E+02	119.7	0.00E+00	1.34E-01			6.43E-14	1.71E-14	2.00E-17	2.69E-18	3
Brain	Structural	Cortical Gray Matter mass	g	2.25E-09	1.043	+/-	0.073		Scaled to whole brain # neuronal cells. Mass from LHH Ref 2.	5.72E+02	105.32	0.00E+00	4.25E-01			7.92E-12	2.50E-12	6.97E-15	1.22E-15	3;5
Brain	Structural	Cortical Surface A	cm^2	1.43E+00	1.059				Scaled to brain mass (g)	3.33E+03		3.77E+00	2.21E+00			4.44E-03	1.47E-03	5.23E-06	9.79E-07	6
Brain	Structural	White Matter Surface A	cm^2	8.88E-07	0.873	+/-	0.102		Scaled to # gray matter neurons	5.74E+02		0.00E+00	1.38E+00			2.96E-09	3.32E-03	1.10E-11	7.98E-06	3
Brain	Structural	Capillary Linear Dimension	um						per neuron	4.60E+01		N/A	4.60E+01			N/A	4.60E+01	N/A	4.60E+01	7
Brain	Structural	Capillary Length Per Neuron (Calculated)	um/neuron						Calculated from total capillary length divided by number of neurons	7.55E+00		N/A	7.55E+00			N/A	7.55E+00	N/A	7.55E+00	
Brain	Structural	Capillary Luminal Diameter	um							3.00E+00		N/A	3.00E+00			N/A	3.00E+00	N/A	3.00E+00	8
Brain	Structural	Total Capillary Length	km						Calculated by length/neuron*# neurons	6.50E+02		N/A	6.50E-01			N/A	6.50E-04	N/A	6.50E-07	8
Brain	Structural	Capillary Volume (resident blood vol)	mL						From LHH source 13	1.00E+00		N/A	1.00E-03			N/A	1.00E-06	N/A	1.00E-09	8
Brain	Structural	Capillary Volume (calculated)	mL						Calculated from diameter and length	4.59E+00		N/A	4.59E-03			N/A	4.59E-06	N/A	4.59E-09	9
Brain	Structural	Total Capillary Volume	uL						131 um^3/neuron X Whole Brain # Neuronal Cells	1.13E+04	1.06E+03	0.00E+00	1.13E+01			0.00E+00	1.13E-02	1.34E-03	1.13E-05	2
Brain	Structural	Cerebrospinal fluid volume	mL							1.60E+02		N/A	1.60E-01				1.60E-04		1.60E-07	10
Brain	Structural	Capillary Surface Area	cm^2/g							1.75E+02	25	N/A	1.75E+02			N/A	1.75E+02	N/A	1.75E+02	4;8;11
Brain	Structural	Capillary Surface Area	m^2						Average of total capillary surface area range from multiple sources 12-18 m^2	1.50E+01	3	N/A	1.50E-02			N/A	1.50E-05	N/A	1.50E-08	4;8;11
Brain	Structural	Total Capillary Surface Area	um^2						174 um^2 per neuron X Whole Brain # Neuronal Cells	1.50E+13		0.00E+00	1.50E+10			0.00E+00	1.50E+07	1.77E+06	1.50E+04	
Brain	Structural	Axonal Cross Sectional Area	um^2	3.69E-01	0.032	+/-	0.049		Essentially invariant for primate brains. Scaled to cortical gray matter # neurons	7.85E-01		0.00E+00	7.58E-01			3.00E-01	7.58E-01	2.44E-01	7.58E-01	3;12
Brain	Structural	Axonal Length	mm		0.662	+/-	0.186		Scaled to cortical radius	NV		N/A	NV			N/A	NV	N/A	NV	3
Brain	Structural	Axonal Length	mm		0.242	+/-	0.085		Scaled to cortical gray matter # neurons	NV		N/A	NV			N/A	NV	N/A	NV	3
Brain	Structural	mitochondrial surface area			0.86				Follows metabolic rate and scales to brain mass											
Brain	Structural	Total cell number	cells							1.70E+11	1.39E+10	0.00E+00	1.70E+08			0.00E+00	1.70E+05	1.06E+04	1.70E+02	1
Brain	Structural	Whole Brain # Neuronal Cells	cells	5.49E+06	0.801				Scaled to body mass	8.61E+10	8.12E+09	0.00E+00	8.61E+07			0.00E+00	8.61E+04	1.02E+04	8.61E+01	1;5
Brain	Structural	Whole Brain # Non-Neuronal Cells	cells	5.49E+06	1				Scaled to body mass	8.46E+10	9.83E+09	0.00E+00	8.46E+07			0.00E+00	8.46E+04	3.84E+02	8.46E+01	1;5
Brain	Structural	Whole Brain: #Non-Neuronal/#Neuronal								9.83E-01		N/A	9.83E-01			N/A	9.83E-01	N/A	9.83E-01	
Brain	Structural	Cerebellum # cells	cells							8.51E+10	6.92E+09	N/A	8.51E+07			N/A	8.51E+04	N/A	8.51E+01	5
Brain	Structural	Cerebellum # Neurons	cells							6.90E+10	6.65E+09	N/A	6.90E+07	4.20E+07		N/A	6.90E+04	N/A	6.90E+01	5
Brain	Structural	Cerebellum # Non-Neuronal	cells							1.60E+10	2.17E+09	N/A	1.60E+07			N/A	1.60E+04	N/A	1.60E+01	5
Brain	Structural	Cerebellum: #Non-Neuronal/#Neuronal								2.32E-01		N/A	2.32E-01			N/A	2.32E-01	N/A	2.32E-01	
Brain	Structural	Cerebral Cortex # cells	cells							7.72E+10	7.72E+09	N/A	7.72E+07			N/A	7.72E+04	N/A	7.72E+01	5
Brain	Structural	Cerebral Cortex # Neurons	cells							1.63E+10	2.17E+09	N/A	1.63E+07	1.30E+07		N/A	1.63E+04	N/A	1.63E+01	5
Brain	Structural	Cerebral Cortex #Non-Neuronal	cells							6.08E+10	7.02E+09	N/A	6.08E+07			N/A	6.08E+04	N/A	6.08E+01	5
Brain	Structural	Cerebral Cortex: #Non-Neuronal/#Neuronal								3.72E+00		N/A	3.72E+00			N/A	3.72E+00	N/A	3.72E+00	
Brain	Structural	Cortical Grey matter # Neurons	cells	1.89E+07	0.911				Scaled to cortical mass	1.24E+10	3.44E+09	0.00E+00	1.24E+07			1.45E-03	1.24E+04	2.40E-06	1.24E+01	5
Brain	Structural	Cortical Grey matter # Non-Neuronal	cells							1.74E+10	1.56E+09	N/A	1.74E+07			N/A	1.74E+04	N/A	1.74E+01	5
Brain	Structural	Cortical Gray Matter: #Non-Neuronal/#Neuronal								1.40E+00		N/A	1.40E+00			N/A	1.40E+00	N/A	1.40E+00	
Brain	Structural	Cortical White Matter # Neurons	cells							2.58E+09	1.08E+09	N/A	2.58E+06			N/A	2.58E+03	N/A	2.58E+00	5

Brain	Structural	Cortical White Matter # Non-Neuronal	cells	6.95E-02	1.165	+/-	0.07		Scaled to cortical gray matter # neurons	3.98E+10	5.66E+09	0.00E+00	3.98E+07			3.44E-05	3.98E+04	1.97E-08	3.98E+01	5
		Cortical White Matter: #Non-Neuronal/#Neuronal								1.54E+01		N/A	1.54E+01			N/A	1.54E+01	N/A	1.54E+01	
Brain	Structural	Rest of Brain # Cells	cells							8.42E+09	1.50E+09	N/A	8.42E+06			N/A	8.42E+03	N/A	8.42E+00	5
Brain	Structural	Rest of Brain # Neurons	cells						<1% total cells	6.90E+08	1.20E+08	N/A	6.90E+05			N/A	6.90E+02	N/A	6.90E-01	5
Brain	Structural	Rest of Brain # Non-Neuronal	cells						RoB = Basal ganglia, diencephalon, brainstem	7.73E+09	1.45E+09	N/A	7.73E+06			N/A	7.73E+03	N/A	7.73E+00	5
Brain	Structural	Rest of Brain: #Non-Neuronal/#Neuronal								1.12E+01		N/A	1.12E+01			N/A	1.12E+01	N/A	1.12E+01	
Brain	Structural	Neocortical # Cells	cells							3.87E+10		N/A	3.87E+07			N/A	3.87E+04	N/A	3.87E+01	13
Brain	Structural	Neocortical # Neurons	cells							1.67E+10		N/A	1.67E+07			N/A	1.67E+04	N/A	1.67E+01	13
Brain	Structural	Neocortical # Glia	cells							1.92E+10		N/A	1.92E+07			N/A	1.92E+04	N/A	1.92E+01	13
Brain	Structural	Neocortical: # Glia/# Neurons								1.15E+00		N/A	1.15E+00			N/A	1.15E+00	N/A	1.15E+00	
Brain	Structural	Neocortical # Vascular Cells	cells							7.73E+09		N/A	7.73E+06			N/A	7.73E+03	N/A	7.73E+00	13
Brain	Structural	Neocortical # Microglia	cells							3.48E+09		N/A	3.48E+06			N/A	3.48E+03	N/A	3.48E+00	13
Brain	Functional	Cell Turnover	%						Scales with Age	1.00E+01										9
Brain	Functional	Cerebral Blood Flow	L/min						13% of total body blood flow	7.00E-01		N/A	7.00E-04			N/A	7.00E-07	N/A	7.00E-10	14
Brain	Functional	Cerebral Blood Flow	mL/100g.min						Agrees with cerebral blood flow in L/min when calculated with brain mass	5.27E+01		N/A	5.27E+01			N/A	5.27E+01	N/A	5.27E+01	15
Brain	Functional	CBF changes with aging							linear regression with age, slope =	-1.18E-01	0.043	N/A	N/A			N/A	N/A	N/A	N/A	16
Brain	Functional	Capillary Shear Stress	Pa	57.13	-1.5779				Max around 10 (microvessels) min around 0.28 (venules). Scaled to capillary diameter	1.54E+00			1.54E+00			N/A	1.54E+00	N/A	1.54E+00	17;18
Brain	Functional	Mean Arterial Blood Pressure	mmHg							8.20E+01		N/A	8.20E+01			N/A	8.20E+01	N/A	8.20E+01	15
Brain	Functional	Cerebral Vascular Resistance	mmHg/100g							1.56E+00		N/A	1.56E+00			N/A	1.56E+00	N/A	1.56E+00	15
Brain	Functional	Arteriovenous Oxygen Difference	volume %							6.10E+00		N/A	6.10E+00			N/A	6.10E+00	N/A	6.10E+00	15
Brain	Functional	Oxygen extraction fraction changes with aging							Linear regression with age, slope =	1.00E-03		N/A	N/A			N/A	N/A	N/A	N/A	
Brain	Functional	Arterial CO2 content	volume %							4.75E+01		N/A	4.75E+01			N/A	4.75E+01	N/A	4.75E+01	15
Brain	Functional	CO2 Partial Pressure	mmHg							3.71E+01		N/A	3.71E+01			N/A	3.71E+01	N/A	3.71E+01	19
Brain	Functional	Conduction Velocity	s^-1		0.242	+/-	0.085		Decreased connectivity as the cortex grows. This decreases the average conduction delay along global connections. Scaled to cortical gray matter # neurons	NV		N/A	NV			N/A	NV	N/A	NV	3
Brain	Functional	Conduction Velocity Primates			0.165				Scaled to cortical gray matter # neurons	NV		N/A	NV			N/A	NV	N/A	NV	3
Brain	Functional	Conduction Velocity Rodents			0.466				Scaled to cortical gray matter # neurons	NV		N/A	NV			N/A	NV	N/A	NV	20
Brain	Functional	Computational Capacity Primates			0.623				Scaled to cortical gray matter # neurons	NV		N/A	NV			N/A	NV	N/A	NV	20
Brain	Functional	Computational capacity Rodents			0.446				Scaled to cortical gray matter # neurons	NV		N/A	NV			N/A	NV	N/A	NV	20
Brain	Structural	Non-Neuronal (Glial) cell density per Neuron			1				Scaled to whole brain # neuronal cells.	NV		N/A	NV			N/A	NV	N/A	NV	21
Brain	Structural	Neuronal Cell Density (Primates)	Neurons/mg		-0.123				Average of two papers +/- Stdev. Scaled to brain mass	NV		N/A	NV			N/A	NV	N/A	NV	21
Brain	Structural	Neuronal Cell Density (Rodents)			-0.367				Scaled to brain mass	NV		N/A	NV			N/A	NV	N/A	NV	21
Brain	Structural	neuronal density with brain mass (all)			-0.172				Scaled to brain mass	NV		N/A	NV			N/A	NV	N/A	NV	21
Brain	Functional	metabolic demand/value range	Metabolic Rate/g		-0.14				Scaled to brain mass	NV		N/A	NV			N/A	NV	N/A	NV	21
Brain	Functional	Whole Brain Glucose Consumption	umol/min	0.785329379	0.873				Across 6 species. Scaled to brain mass	4.68E+02		1.75E+00	2.05E-01	3.70E-01		6.72E-03	2.05E+02	2.59E-05	2.05E+05	21
Brain	Functional	Glucose consumption per mass	umol/g.min	0.785329547	-0.127				Across 6 species. Scaled to brain mass	3.10E-01		6.99E-01	3.10E-01	8.90E-01		1.57E+00	3.10E-01	3.52E+00	3.10E-01	21
	Functional	Glucose per neuron	umol/min		1				Calculated from whole brain glucose consumption divided by number of neurons	5.44E-09			5.44E-09				5.44E-09		5.44E-09	
Brain	Functional	Whole Brain Oxygen Consumption	mL/min	0.092281743	0.862				Across 6 species, human number average of 2 sources +/- Stdev. Scaled to brain mass.	5.07E+01	2.1	2.03E-01	5.28E-02	1.90E-01		8.39E-04	5.28E-05	2.59E-05	8.85E-07	10;21
Brain	Functional	Whole Brain Oxygen Consumption	mL/g.min						For humans, calculated from whole brain oxygen consumption divided by organ mass	3.50E-02	0.005	8.13E-02	3.50E-02	0.084 (rat)		1.96E-01	3.50E-02	3.52E+00	3.50E-02	10
Brain	Functional	Cerebral Cortex Glucose Consumption	umol/g.min							3.40E-01	0.05	N/A	3.40E-01	1.10E+00		N/A	3.40E-01	N/A	3.40E-01	10
Brain	Functional	Cerebral Metabolic Rate (oxygen/mass)	mL/100g.min							3.21E+00		N/A	3.21E+00			N/A	3.21E+00	N/A	3.21E+00	15
Brain	Functional	CMRO2 changes with aging							Linear regression with age, slope =	-2.40E-01	0.05									16
Brain	Functional	Firing Rate			-0.15				Also differs for type of neuron. Scaled to body mass	1-40 Hz			1-40 Hz				1-40 Hz		1-40 Hz	10
Heart																						Heart
Heart	Structural	Organ Weight	g	5.05E+00	0.98				w/o blood	2.55E+02	± 2.40E+01	3.73E-01	2.55E-01	1.50E-01	± 5.00E-02	4.28E-04	2.55E-04	4.92E-07	2.55E-07	22;23
Heart	Structural	Organ Volume	L	4.21E-03	1.00					2.95E-01	± 1.50E-02	2.95E-04	2.95E-04	9.50E-05		2.95E-07	2.95E-07	2.95E-10	2.95E-13	14
Heart	Structural	Organ Mean Linear Dimension	cm	3.25E+00	0.33					13.5	1.5	1.35E+00	1.35E+00	1 cm		1.38E-01	1.35E-01	1.41E-02	1.35E-02	23;24
Heart	Structural	LV Weight	g	3.51E+00	0.98					1.78E+02	± 4.40E+01	2.59E-01	1.78E-01	9.10E-02	± 2.00E-02	2.97E-04	1.78E-04	3.41E-07	1.78E-07	25
Heart	Structural	LV Wall Thickness	mm	1.80E+00	0.33					7.5	2.5	7.50E-01	7.50E-01	1.50E+00		7.67E-02	7.50E-02	7.85E-03	7.50E-03	26;27
Heart	Structural	LV Wall Thickness	cells	3.61E+01	0.33					150	30	1.50E+01	1.50E+01	150 (rat)		1.53E+00	1-2	1.57E-01	1.00E+00	28;29
Heart	Structural	LV Surface Area	cm^2	1.32E+01	0.67				Ranges from 180-260 cm^2	2.23E+02	± 3.75E+01	2.23E+00	2.23E+00	1.00E+00		2.17E-02	2.17E-02	2.12E-04	2.17E-04	30;31
Heart	Structural	LV Radii	mm	7.73E+00	0.33					3.22E+01	± 2.25E-01	3.22E+00	3.22E+00	5.15 (rat)		3.29E-01	3.22E-01	3.37E-02	3.22E-02	32
Heart	Structural	LV Radius of Curvature	mm	8.45E+04	3					2.90E+00		2.90E+01	2.90E+01	19.4 (rat)		2.90E-08	2.90E+02	2.90E-17	2.90E+03	33
Heart	Structural	Resident Vascular Blood Volume	L	3.83E-04	1.00				~10.5 mL/100g of tissue	2.68E-02		2.68E-05	2.68E-05	2.84E-05		2.68E-08	2.68E-08	2.68E-11	2.68E-11	34;35

Heart	Structural	End Diastolic Vlood Volume	mL	1.71E+00	1.00		1.20E+02		1.20E-01	1.20E-01	6.00E-02		1.20E-04	1.20E-04	1.20E-07	1.20E-07	36;37
Heart	Functional	Perfusion Rate	L/ min	9.92E-03	0.75		2.40E-01		1.35E-03	2.40E-04	2.80E-04		7.59E-06	2.40E-07	4.27E-08	2.40E-10	14
Heart	Structural	Total Cell Number	cells	N/A	N/A	Using 20,000,000 cells/cm^3	5.90E+09			5.90E+06	2.81E+06		N/A	5.90E+03	N/A	5.60E+00	38
Heart	Structural	Mass Per Cell	g	N/A	N/A		4.32E-08			4.32E-08	5.34E-08		N/A	4.32E-08	N/A	4.32E-08	
Heart	Structural	Cell Density	$cells/cm^3$	N/A	N/A		2.00E+07			2.00E+07	5.80E+07		N/A	2.00E+07	N/A	monolayer	29;39
Heart	Structural	Number of Important Cell Types	cell types	N/A	N/A	Cardiomyocytes, Fibroblasts, VSMCs, ECs, neurons	5.00E+00			5.00E+00	5.00E+00		N/A	1-2	N/A	1.00E+00	
Heart	Functional	Cell Turnover Rate	new cells (yr^{-1})	N/A	N/A	1% turnover at 25, 0.45% turnover at 75 years (calculated assuming 1% turnover)	5.90E+07		N/A	5.90E+04	1.41E+01		N/A	5.90E+01	N/A	5.60E-02	40;41
Heart	Functional	Fractional Cell Shortening	um/cell	N/A	N/A		1.05E+01			1.05E+01	4.14E+00		N/A	1.05E+01	N/A	1.05E+01	27;42;43
Heart	Metabolic	MVO_2	ml O_2/100g/min	4.13E-01	0.75		1.00E+01	± 3.00E+00	5.62E-02	1.00E+01	8.30E-01	± 1.20E-01	3.16E-04	1.00E+01	1.78E-06	1.00E+01	44;45
Heart	Functional	Total Transport Capacity	mL/min	2.17E+02	0.75		5.25E+03	± 9.75E+02	2.95E+01	5.25E+00	2.00E+01	± 5.00E+00	1.66E-01	5.25E-03	9.34E-04	5.25E-06	46;47
Heart	Functional	Ejection Fraction	%				6.25E-01	± 7.50E-02		6.25E+01	6.60E+01	± 4.00E+00	N/A	6.25E-01	N/A	6.25E-01	37;48
Heart	Functional	Oscillatory Frequency	bpm	2.02E+02	-0.25		6.50E+01		3.93E+02	6.50E+01	6.32E+02	± 5.68E+01	2.21E+03	6.50E+01	1.24E+04	6.50E+01	49
Heart	Functional	Wall Shear Stress	$dynes/cm^2$	1.66E+01	-0.20	Experimental: -0.2027; Theoretical: -0.375	7.00E+00		2.84E+01	7.00E+00	3.50E+01		1.15E+02	7.00E+00	4.67E+02	7.00E+00	50
Heart	Metabolic	Max O2 Consumption nmol/mm^3/s	nmol/mm^3/s	N/A	N/A	Human value is average *at rest* (250 mL O_2 min^{-1})	5.55E-01				7.00E-01						22
Heart	Structural	Capillary Density	capillaries/mm^2	N/A	N/A	in children and adults, higher density in infants	2.39E+03	± 7.50E+01			2.25E+03	± 8.50E+01					22
Heart	Structural	Myocyte Fractional area	%	N/A	N/A		1.20E+01	± 5.90E+00			8.21E+01	± 9.00E-01					22
Heart	Metabolic	Max MVO2 Calculation	mL O2/100g/min	N/A	N/A	in men	5.59E+01				6.77E+01						22
Heart	Structural	% Mitochondria (v/v)		N/A	N/A	% of CM cytosolic volume	2.53E-01				3.80E-01						45
Kidney																	Kidney
Kidney	Structural	Kidney Mass	g			Mass from literature	3.10E+02				3.20E-01						14
Kidney	Structural	Kidney Mass	g	2.12E-02	0.85	Mass from allometric scaling	2.78E+02		7.85E-01		2.71E-01		2.21E-03		6.23E-06		51-54
Kidney	Structural	Kidney Volume	mL			Volume from literature	2.80E+02				3.40E-01						14
Kidney	Structural	Kidney Volume	mL	2.18E-02	0.84	Volume from allometric scaling	2.65E+02		7.83E-01		2.72E-01		2.32E-03		6.85E-06		55
Kidney	Structural	Cortical Thickness	mm	2.62E+00	0.17		5.39E+00		1.67E+00		1.35E+00		5.15E-01		1.59E-01		56
Kidney	Structural	Medullary Thickness	mm	8.15E+00	0.13		1.41E+01		5.78E+00		4.92E+00		2.37E+00		9.73E-01		57
Kidney	Structural	Outer Medullary Thickness	mm	3.17E+00	0.18		6.81E+00		1.96E+00		1.57E+00		5.66E-01		1.63E-01		56
Kidney	Structural	Inner Medullary Thickness	mm	5.09E+00	0.14		9.23E+00		3.51E+00		2.94E+00		1.33E+00		5.07E-01		56
Kidney	Structural	Loop Length	um	1.85E+03	1.02		0.00E+00		0		0		0		0		57
Kidney	Structural	Renal Blood Flow (RBF)	mL/min			Renal Blood Flow from literature	1.24E+03				1.30E+00						14
Kidney	Structural	Renal Blood Flow (RBF)	mL/min	4.31E+01	0.77	Renal Blood Flow from allometric scaling	1.13E+03		5.56E+00		2.12E+00		2.72E-02		1.33E-04		58
Kidney	Structural	Plasma Flow Rate (PFR)	mL/min			Plasma Flow Rate from literature	7.00E+02				8.00E-01						55
Kidney	Structural	Plasma Flow Rate (PFR)	mL/min	8.45E-02	0.80	Plasma Flow Rate from allometric scaling	6.50E+02		2.55E+00		9.34E-01		1.00E-02		3.93E-05		55
Kidney	Structural	# Nephrons, Both Kidneys		1.88E+05	0.62		2.62E+06		3.62E+04		1.66E+04		4.99E+02		6.89E+00		52;53;55
Kidney	Structural	# Glomeruli, Both Kidneys		1.91E+05	0.62		2.66E+06		3.67E+04		1.69E+04		5.06E+02		6.98E+00		59
Kidney	Structural	# Nephrons/g of Kidney		3.24E+04	-0.32		8.32E+03		7.59E+04		1.13E+05		6.92E+05		6.31E+06		59
Kidney	Structural	Glomerular Surface/g of Kidney	mm^2	2.81E+03	-0.15		1.49E+03		4.19E+03		5.05E+03		1.18E+04		3.32E+04		59
Kidney	Structural	Total Glomerular Volume	mL	1.37E-01	0.85		5.07E+00		1.43E-02		4.93E-03		4.03E-05		1.14E-07		53;59
Kidney	Structural	Total Glomerular SA	mm^2	8.37E+03	0.73		1.86E+05		1.20E+03		4.81E+02		7.76E+00		5.01E-02		59
Kidney	Structural	SA/Glomerulus	mm^2	8.60E-02	0.18		1.85E-01		5.33E-02		4.25E-02		1.54E-02		4.43E-03		59
Kidney	Structural	Proximal Tubule Length	mm	1.43E+01	0.10		2.19E+01		1.10E+01		9.69E+00		5.50E+00		2.76E+00		59
Kidney	Structural	Proximal Tubule Diameter	mm	6.00E-02	0.02		6.53E-02		5.69E-02		5.55E-02		4.96E-02		4.32E-02		59
Kidney	Structural	Proximal Tubule Volume	mm^3	4.60E-02	0.12		7.66E-02		3.34E-02		2.88E-02		1.46E-02		6.37E-03		59
Kidney	Structural	Total of Proximal Tubule Volumes	mm^3	4.28E+03	0.68		7.70E+04		7.02E+02		3.00E+02		6.40E+00		5.84E-02		59
Kidney	Structural	Proximal Tubule Volume/g of Kidney	mm^3	1.47E+03	-0.20		6.29E+02		2.51E+03		3.22E+03		9.97E+03		3.97E+04		59
Kidney	Structural	Mean Glomerular Diameter	um	6.10E+01	0.11		2.08E+02		9.73E+01		8.48E+01		0.00E+00		2.13E+01		54
Kidney	Functional	Glomerular Filtration Rate (GFR)	mL/min				1.25E+02			1.25E-01	2.80E-01			1.25E-04			14
Kidney	Functional	Glomerular Filtration Rate (GFR)	mL/min	5.36E+00	0.72		1.14E+02		7.90E-01		3.21E-01		5.47E-03		3.78E-05		60
Kidney	Functional	Single Nephron GFR	nL/min	2.80E+01	0.10		4.28E+01		2.15E+01		1.89E+01		1.08E+01		5.39E+00		53
Kidney	Functional	Urine Flow	mL/day			Urine Flow from literature	1.40E+03				1.00E+00						14
Kidney	Functional	Urine Flow	mL/day	6.09E+01	0.75	Urine Flow from allometric scaling	1.47E+03		8.28E+00		3.24E+00		4.66E-02		2.62E-04		58
Kidney	Functional	Urinary Concentrating Ability (*#4)	mmol/kgH2O	2.67E+03	-0.10		1.77E+03		3.45E+03		3.90E+03		6.75E+03		1.32E+04		56;57
Kidney	Functional	Clearance			0.75												53
Kidney	Functional	Clearance, Urea	mL/hr	1.59E+00	0.72		3.39E+01		2.34E-01		9.51E-02		1.62E-03		1.12E-05		52;55
Kidney	Functional	Clearance, Inulin	mL/min	5.36E+00	0.72		1.14E+02		7.90E-01	1.14E-01	3.21E-01		5.47E-03	1.14E-04	3.78E-05		53;58
Kidney	Functional	Clearance, Creatinine	mL/min	8.20E+00	0.69		1.54E+02		1.31E+00		5.51E-01		1.11E-02		9.48E-05		52;55;61
Kidney	Functional	Clearance, Methotrexate (MTX)	mL/min	1.09E+01	0.69		2.04E+02		1.74E+00		7.33E-01		1.48E-02		1.26E-04		61
Kidney	Functional	Clearance, Para-aminohippurate (PAH)	mL/min	2.18E+01	0.77		5.74E+02		2.81E+00		1.07E+00		1.38E-02		6.75E-05		58
Kidney	Functional	Excretion, Urinary Nitrogen	mg/day	1.46E+02	0.72		3.11E+03		2.15E+01		8.73E+00		1.49E-01		1.03E-03		60
Kidney	Functional	Excretion, Creatinine Nitrogen	mg/day	1.27E+01	0.90		5.71E+02		1.17E+00		3.82E-01		2.40E-03		4.93E-06		60
Kidney	Functional	Excretion, Neutral Sulfur	mg/day	6.85E+00	0.74		1.59E+02		9.57E-01		3.79E-01		5.77E-03		3.48E-05		60
Kidney	Metabolic	Species Basal Metabolic Rate	W	3.89E+00	0.76		9.82E+01		5.15E-01		1.99E-01		2.71E-03		1.42E-05		57
Kidney	Metabolic	Species Mass Specific Metablic Rate	W/kg	3.89E+00	-0.24		1.40E+00		7.36E+00		9.95E+00		3.86E+01		2.03E+02		57
Kidney	Metabolic	Kidney Mass Specific Metabolic Rate	kJ kg-1 day-1	2.89E+03	-0.08		2.06E+03		3.57E+03		3.95E+03		6.21E+03		1.08E+04		51;62
Kidney	Metabolic	Mass Specific Oxygen Consumption			-0.10												63
Kidney	Metabolic	Mitochondrial Volume Density (% of cell vol)	%	3.80E+01	-0.14		7.96E+00		2.09E+01		2.50E+01		5.51E+01		1.45E+02		64

Kidney	Metabolic	Mitochondrial Membrane SA (m^2) per cm^3 Tissue	m^2/cm^3	2.17E+01	-0.22					1.87E+00			8.53E+00			1.12E+01			3.90E+01			1.78E+02			64
Kidney	Metabolic	Vol Mitochondria/mTAL Cell Vol	%	5.62E+01	-0.06					4.43E+01			6.53E+01			7.00E+01			9.61E+01			1.41E+02			63
Kidney	Metabolic	Inner Mitochondial Membrane Area/Vol mTAL Mito	um^-1	4.90E+01	-0.03					4.24E+01			5.36E+01			5.59E+01			6.78E+01			8.58E+01			63
Kidney	Metabolic	Inner Mitochondial Membrane Area/mTAL Cell Vol	um^-1	2.75E+01	-0.09					1.86E+01			3.52E+01			3.95E+01			6.64E+01			1.25E+02			63
Kidney	Metabolic	Basolateral Membrane Area/mTAL Cell Vol	um^-1	5.50E+00	-0.08					4.00E+00			6.71E+00			7.38E+00			1.13E+01			1.89E+01			63
Liver																									Liver
Liver	Structural	Organ Weight	g	3.70E-02	0.85					1.52E+03			1.36E+00	1.52E+00		1.50E+00			3.87E-03	1.52E-03		1.10E-05	1.52E-06		65
Liver	Structural	Organ Volume	mL							1.69E+03				1.69E+00		1.30E+00				1.69E-03			1.69E-06		14
Liver	Metabolic	Oxygen Consumption	mL/min	3.50E-02	0.69					2.07E+03			6.56E-01	2.07E+00					5.59E-03			4.76E-05			65;67
Liver	Functional	Blood Flow	mL/min	9.40E-02	0.75					1.45E+03			2.27E+00	1.45E+00					1.28E-02	1.45E-03		7.19E-05	1.45E-06		14;65
Liver	Structural	Resident Blood Volume	mL	2.50E-02	0.86								9.65E-01						2.54E-03			6.68E-06			65
Liver	Functional	Bile Flow	mL/day							3.50E+02				3.50E-01		2.00E+00				3.50E-04			3.50E-07		14
Liver	Structural	Hepatocytes	cells	9.10E+06	0.89					3.00E+11			3.92E+08	3.00E+08					8.63E+05	3.00E+05		1.90E+03	3.00E+02		65
Liver	Structural	Hepatocyte Cell Density	cells/g liver							1.39E+08	±	2.50E+07		1.39E+05		1.35E+02	±	1.00E+01		1.39E+02			1.39E-01		68
Liver	Functional	Protein Concentration	mg/g liver							9.00E+01	±	1.70E+01		9.00E-02		1.15E+02	±	7.00E+00		9.00E-05			9.00E-08		68
Liver	Structural	Liver Density	g liver/mL							1.03E+00				1.03E-03						1.03E-06			1.03E-09		14
Liver	Functional	Potassium Uptake Rate	µmol K+/g wet * min	1.20E+00	-0.14								6.62E-01						1.74E+00			4.58E+00			69
Liver	Metabolic	Tissue Metabolic Rate (Oxygen)	µmol O2/g wet * min	3.60E+00	-0.21								1.48E+00						6.29E+00			2.68E+01			69
Liver	Functional	Shear Stress	MPa						Liver sinusoid	5.00E+01				5.00E-02						5.00E-05			5.00E-08		70
Liver	Functional	CI, intrinsic																							
Liver	Functional	Antipyrine	mL/min	5.00E-02	1.84				Corrected with brain weight	3.43E+02			3.75E-04	3.43E-01					1.13E-09	3.43E-04		3.42E-15	3.43E-07		71
Liver	Functional	Caffeine	mL/min	7.00E-02	1.53				Corrected with brain weight	1.40E+02			1.20E-03	1.40E-01					3.08E-08	1.40E-04		7.91E-13	1.40E-07		71
Liver	Functional	Mibefradil	mL/min	3.63E+01	1.31				Corrected with brain weight	4.90E+02			1.11E+00	4.90E-01					1.31E-04	4.90E-04		1.54E-08	4.90E-07		71
Liver	Functional	Moforotene	mL/min	1.00E+02	1.64				Corrected with brain weight	7.70E+02			1.28E+00	7.70E-01					1.53E-05	7.70E-04		1.84E-10	7.70E-07		71
Liver	Functional	Theophylline	mL/min	3.00E-02	1.71				Corrected with brain weight	4.27E+01			3.18E-04	4.27E-02					2.36E-09	4.27E-05		1.75E-14	4.27E-08		71
Liver	Functional	Tolcapone	mL/min	1.03E+02	1.51				Corrected with brain weight	1.89E+02			1.86E+00	1.89E-01					5.48E-05	1.89E-04		1.62E-09	1.89E-07		71
Liver	Functional	Bromazepam	mL/min						Adjusted from reference weight to 70kg human	6.78E+01															61
Liver	Functional	Clonazepam	mL/min						Adjusted from reference weight to 70kg human	4.28E+02															61
Liver	Functional	Chlordiazepoxide	mL/min						Adjusted from reference weight to 70kg human	4.46E+02															61
Liver	Functional	Antipyrine	mL/min	8.16E+00	0.89								7.76E-01						1.32E-02			2.91E-05			66
Liver	Functional	Phenytoin	mL/min	4.71E+01	0.92								4.13E+00						4.13E+00			7.44E-03			66
Lung																									Lung
Lung	Structural								***averaged values - Reported**							***averaged**									
Lung	Structural	Total Lung Capacity (TLC)	mL	5.35E+01	1.06	70 kg human .25 kg rat				5.50E+03	±	5.00E+02	3.19E+00	5.50E+00		9.50E+00			2.11E-03	5.50E-03		1.39E-06	5.50E-06		72
Lung	Structural	Functional Residual Capacity (FRC)	mL	2.41E+01	1.13	70 kg human .25 kg rat				3.05E+03	±	6.50E+02	1.19E+00	3.05E+00		1.50E+00			4.86E-04	3.05E-03		1.98E-07	3.05E-06		72
Lung	Structural	Tidal Volume	mL	7.69E+00	1.04	70 kg human .25 kg rat				4.50E+02	±	5.00E+01	4.84E-01	4.50E-01		1.65E+00			3.67E-04	4.50E-04		2.79E-07	4.50E-07		72
Lung	Structural	Dead Space	mL	2.76E+00	0.96	70 kg human .25 kg rat				1.50E+02	±	0.00E+00	2.15E-01	1.50E-01		7.90E-01			2.83E-04	1.50E-04		3.73E-07	1.50E-07		72
Lung	Functional	Frequency of Respiration	min-1	5.35E+01	-0.26	70 kg human .25 kg rat				1.65E+01	±	5.50E+00	1.07E+02	1.65E-02		1.06E+02			6.44E+02	1.65E-05		3.88E+03	1.65E-08		72
Lung	Functional	Minute Volume (ml/min)	mL/min	3.79E+02	0.80	70 kg human .25 kg rat				6.50E+03	±	5.00E+02	4.52E+01	6.50E+00		2.00E-01			1.80E-01	6.50E-03		7.16E-04	6.50E-06		72
Lung	Functional	Lung Compliance	mL/cm H2O	2.10E+00	1.08	70 kg human .25 kg rat				1.63E+02	±	3.75E+01	1.19E-01	1.63E-01		4.50E-01			6.84E-05	1.63E-04		3.93E-08	1.63E-07		72
Lung	Functional	Flow Resistance	cm H2O/(L/sec)	2.44E+01	-0.70	70 kg human .25 kg rat				1.40E+00	±	5.00E-01	1.57E+02	1.40E-03		9.50E+01			1.98E+04	1.40E-06		2.49E+06	1.40E-09		72
Lung	Functional	Diffusion Capacity CO	mL/mmHg/min	2.20E-01	1.14	70 kg human .25 kg rat				3.35E+01	±	1.65E+01	1.06E-02	3.35E-02		4.50E-02			4.03E-06	3.35E-05		1.53E-09	3.35E-08		72
Lung	Functional	Power of Breathing	g*cm/min	9.62E+02	0.78	70 kg human .25 kg rat				4.00E+04	±	1.00E+04	1.21E+02	4.00E+01		6.25E+02			5.53E-01	4.00E-02		2.53E-03	4.00E-05		
Lung	Structural	Organ Weight	g	1.13E+01	0.99	70 kg human .25 kg rat				1.00E+03			8.12E-01			1.50E+00			8.70E-04	1.00E-03		9.33E-07	1.00E-06		72
Lung	Structural	Acinar Diameter	cm	4.20E-02	0.17	70 kg human .25 kg rat				2.86E-01			2.66E-02	2.86E-04		7.40E-02			8.10E-03	2.86E-07		2.47E-03	2.86E-10		73
Lung	Structural	Terminal Bronchiole Diameter	cm	5.20E-03	0.21	70 kg human .25 kg rat				4.40E-02			2.97E-03	4.40E-05		4.10E-03			6.97E-04	4.40E-08		1.63E-04	4.40E-11		73

Lung	Structural	Alveolar Diameter	cm	3.10E-03	0.15	70 kg human .25 kg rat		1.82E-02		2.07E-03	1.82E-05	4.48E-03		7.31E-04	1.82E-08	2.58E-04	1.82E-11	73
Lung	Structural	Surface Area Alveolar Epithelium	m^2		X	70 kg human, 20 g mouse		1.02E+02 ± 2.05E+01			1.02E-01	5.00E-02 ± 2.00E-02			1.02E-04		1.02E-07	74
Lung	Structural	Surface Area Type 1 Epithelium	m^2		X	70 kg human, 20 g mouse		9.60E+01 ± 1.91E+01			9.60E-02	5.00E-02 ± 2.00E-02			9.60E-05		9.60E-08	74
Lung	Structural	Surface Area Type 2 Epithelium	m^2		X	70 kg human, 20 g mouse		6.20E+00 ± 1.50E+00			6.20E-03	1.00E-03 ± 2.00E-04			6.20E-06		6.20E-09	74
Lung	Structural	Capillary Endothelium	m^2		X	70 kg human, 20 g mouse		7.23E+01 ± 1.65E+01			7.23E-02	4.00E-02 ± 1.00E-02			7.23E-05		7.23E-08	74
Lung	Structural	Total Alveolar Septal Tissue Volume	cm^3		X	70 kg human, 20 g mouse		2.30E+02 ± 3.80E+01			2.30E-01	6.30E-02 ± 1.20E-02			2.30E-04		1.02E-07	74
Lung	Structural	Type 1 Cell Volume	cm^3		X	70 kg human, 20 g mouse		3.39E+01 ± 3.39E+01			3.39E-02	1.40E-02 ± 3.00E-03			3.39E-05		9.60E-08	74
Lung	Structural	Type 2 Cell Volume	cm^3		X	70 kg human, 20 g mouse		2.23E+01 ± 2.23E+01			2.23E-02	5.00E-03 ± 1.00E-03			2.23E-05		6.20E-09	74
Lung	Structural	Interstitial Cell Volume	cm^3		X	70 kg human, 20 g mouse		3.84E+01 ± 3.84E+01			3.84E-02	1.30E-02 ± 4.00E-03			3.84E-05		7.23E-08	74
Lung	Structural	Interstitial Matrix Volume	cm^3		X	70 kg human, 20 g mouse		8.55E+01 ± 1.06E+01			8.55E-02	7.00E-03 ± 2.00E-03			8.55E-05		2.30E-07	74
Lung	Structural	Endothelial Cell Volume	cm^3		X	70 kg human, 20 g mouse		4.14E+01 ± 1.28E+01			4.14E-02	2.20E-02 ± 3.00E-03			4.14E-05		3.39E-08	74
Lung	Structural	Alveolar Macrophage Volume	cm^3		X	70 kg human, 20 g mouse		8.20E+00 ± 3.10E+00			8.20E-03	1.30E-03 ± 2.00E-04			8.20E-06		2.30E-07	74
Lung	Structural	Total cell number			1.00	69 kg human, 19.2 g mouse	cell number increases proportionally with body mass	1.84E+11 ± 6.40E+10			1.84E+08	1.19E+08 ± 2.70E+07			1.84E+05		1.84E+02	74
Lung	Structural	Type 1 Epithelial Cell Number			1.00	69 kg human, 19.2 g mouse	cell number increases proportionally with body mass	1.96E+10 ± 9.00E+03			1.96E+07	1.16E+07 ± 3.60E+06			1.96E+04		1.96E+01	74
Lung	Structural	Type 2 Epithelial Cell Number			1.00	69 kg human, 19.2 g mouse	cell number increases proportionally with body mass	3.29E+10 ± 1.36E+10			3.29E+07	1.48E+07 ± 3.90E+06			3.29E+04		3.29E+01	74
Lung	Structural	Interstitial Cell Number			1.00	69 kg human, 19.2 g mouse	cell number increases proportionally with body mass	5.25E+10 ± 1.18E+10			5.25E+07	2.69E+07 ± 3.60E+06			5.25E+04		5.25E+01	74
Lung	Structural	Endothelial Cell Number			1.00	69 kg human, 19.2 g mouse	cell number increases proportionally with body mass	7.32E+10 ± 2.88E+10			7.32E+07	6.28E+07 ± 1.53E+07			7.32E+04		7.32E+01	74
Lung	Structural	Alveolar Macrophages Number			1.00	69 kg human, 19.2 g mouse	cell number increases proportionally with body mass	5.99E+09 ± 1.90E+09			5.99E+06	2.90E+06 ± 5.00E+05			5.99E+03		5.99E+00	74
Lung	Structural	Tracheal Radius	cm	N/A	0.39		Theoretical: 0.375 Experimental: 0.39	2.50E+00			2.50E-03				2.50E-06		2.50E-09	75
Lung	Structural	Volume of Alveolus	μm^3	N/A	0.25		Theoretical: 0.25 (assuming sphere and radius of 100 um)	4.19E+06			4.19E+03				4.19E+00		4.19E-03	75
Lung	Structural	Number of Alveoli		N/A	0.75		Theoretical: 0.75	4.00E+08 ± 1.00E+08			4.00E+05				4.00E+02		4.00E-01	75
Lung	Structural	Area of Alveolus	μm^2	N/A	0.17		Theoretical: 0.167 (assuming sphere and radius of 100 um)	1.26E+05			1.26E+02				1.26E-01		1.26E-04	75
Lung	Structural	Area of Lungs	m^2	N/A	0.95		Theoretical: 0.92 Experimental: 0.95	7.00E+01			7.00E-02				7.00E-05		7.00E-08	75
Lung	Metabolic	O2 Consumption Rate	mL/hr/g	N/A	0.75		Theoretical: 0.75 Experimental: 0.76	2.00E-01			2.00E-04	8.40E-01			2.00E-07		2.00E-10	75
Blood																		Blood
Blood	Structural	Volume	mL	7.60E-02	1.00		p value<.001	4.85E+03 ± 1.50E+02		5.32E-03	4.85E+00	2.00E+00 ± 5.00E-01		5.32E-06	4.85E-03	5.32E-09	4.85E-06	61;76
Blood	Structural	Albumin	g/L	5.68E+00	0.30		p value<.01	4.50E+01 ± 1.00E+01		2.59E+00	4.50E+01	2.75E+01 ± 2.50E+00		3.35E-01	4.50E+01	4.33E-02	4.50E+01	61
Blood	Structural	Creatinine	umol/L	5.83E+01	0.14		p value<.001	8.90E+01 ± 2.90E+01		3.99E+01	8.90E+01	4.86E+01 ± 3.09E+01		1.48E+01	8.90E+01	5.53E+00	8.90E+01	77-79
Blood	Structural	K+	mmol/L	5.20E+00	-0.03		p value<.001	4.80E+00 ± 1.30E+00		5.66E+00	4.80E+00	6.25E+00 ± 1.25E+00		7.06E+00	4.80E+00	8.81E+00	4.80E+00	77;78;80
Blood	Structural	Urea	mmol/L	7.30E+00	-0.08		p value<.001	4.10E+00 ± 2.90E+00		9.10E+00	4.10E+00	3.41E+00 ± 2.08E+00		1.62E+01	4.10E+00	2.87E+01	4.10E+00	77-79
Blood	Structural	Hematocrit	% Volume	4.21E+01	-0.02		p value<.001	5.05E+01 ± 1.15E+01		4.45E+01	5.05E+01	4.40E+01 ± 5.00E+00		5.15E+01	5.05E+01	5.95E+01	5.05E+01	77;78;81
Blood	Structural	Hemoglobin	g/L	1.44E+02	-0.02		p value<.001	1.53E+02 ± 2.25E+01		1.53E+02	1.53E+02	1.34E+02 ± 3.20E+01		1.81E+02	1.53E+02	2.14E+02	1.53E+02	77;78;81
Blood	Structural	Glucose	mmol/L	6.40E+00	-0.05		p value<.001	4.95E+00 ± 1.15E+00		7.25E+00	4.95E+00	6.58E+00 ± 3.14E+00		1.00E+01	4.95E+00	1.39E+01	4.95E+00	77-79
Blood	Structural	Triglycerides	mmol/L	9.00E-01	-0.14		p value<.001	9.00E-01 ± 3.00E-01		1.29E+00	9.00E-01	9.22E-01 ± 2.40E-01		3.27E+00	9.00E-01	8.32E+00	9.00E-01	77-79
Blood	Structural	Total Protein	g/L	6.43E+01	0.01		p value= 0.011	7.20E+01 ± 1.20E+01		6.21E+01	7.20E+01	5.35E+01 ± 1.85E+01		5.68E+01	7.20E+01	5.19E+01	7.20E+01	77-79
Blood	Structural	Ca2+	mmol/L	2.60E+00	-0.01		p value=0.034	1.17E+00 ± 1.35E-01		2.67E+00	1.17E+00	2.15E+00 ± 3.70E-01		2.86E+00	1.17E+00	3.07E+00	1.17E+00	77;78
Blood	Structural	Na+	mmol/L	1.46E+02	0.00		p value=0.039	1.41E+02 ± 6.00E+00		1.47E+02	1.41E+02	1.50E+02 ± 1.00E+01		1.51E+02	1.41E+02	1.55E+02	1.41E+02	77;78
Blood	Structural	Phospohorus	mmol/L	1.90E+00	-0.02		p value=0.118	1.25E+00 ± 2.50E-01		2.00E+00	1.25E+00	2.41E+00 ± 5.65E-01		2.30E+00	1.25E+00	2.64E+00	1.25E+00	77;78;81

Blood	Structural	Cl-	mmol/L	1.05E+02	-0.01	p value=0.299	1.03E+02	± 7.50E+00	1.07E+02	1.03E+02	9.90E+01	± 1.10E+01	1.13E+02	1.03E+02	1.19E+02	1.03E+02	77;78
Blood	Structural	Total Bilirubin	umol/L	4.20E+00	-0.09	p value=0.528	1.34E+01	± 1.17E+01	5.32E+00	1.34E+01	7.70E+00	± 7.70E+00	9.84E+00	1.34E+01	1.82E+01	1.34E+01	77;78;81
Blood	Structural	Mg2+	mmol/L	9.00E-01	-0.03	p value=0.721	1.90E+00	± 4.00E-01	9.64E-01	1.90E+00	2.35E+00	± 1.55E+00	1.15E+00	1.90E+00	1.38E+00	1.90E+00	77;78;82
Blood	Structural	Cholesterol	mmol/L	2.70E+00	-0.04	p value=0.774	4.75E+00	± 1.75E+00	3.00E+00	4.75E+00	2.88E+00	± 6.70E-01	3.96E+00	4.75E+00	5.22E+00	4.75E+00	77-79
Blood	Functional	Wall Shear Stress Along the Infrarenal Aorta**	dyn/cm^2	2.60E+00	-0.38	p value<.05	4.80E+00	± 3.00E-01	7.14E+00	4.80E+00	8.76E+01	± 8.30E+00	9.86E+01	4.80E+00	1.36E+03	4.80E+00	83

Blood	Functional	**Oxygen Carriers**	**Relative oxygen capacity**	**α (mL O2/(mL B *atm)) at 37 C**	**Oxygen binding capacity (mL O2/g)**	**Oxygen Diffusivity *10^9 (m^2/s)**									Blood O2 Carriers
Blood	Functional	Water	1	2.39E-02	-	2.89									84;85
Blood	Functional	Hemoglobin	70	3.30E-02	1.37	0.838									85
Blood	Functional	Perfluorocarbon	20	3.50E-01	-	8.29									86;87
Blood	Functional	Blood	70	2.23E-02	-	1.33									85

NOTES

1 In certain cases, the literature values for the allometric scaling laws were for body mass in units other than kg, and hence have been scaled for consistency

Literature Cited

1 Herculano-Houzel,S. The Human Brain in Numbers: a Linearly Scaled-Up Primate Brain, Front.Hum.Neurosci., 3, Article 31 2009
2 Im,K, Lee,JM, Lyttelton,O, Kim,SH, Evans,AC, Kim,SI. Brain Size and Cortical Structure in the Adult Human Brain, Cerebral Cortex, 18, 2181-2191, 2008
3 Herculano-Houzel,S, Mota,B, Wong,PY, Kaas,JH. Connectivity-Driven White Matter Scaling and Folding in Primate Cerebral Cortex, PNAS (US), 107, 19008-19013, 2010
4 Begley,DJ. Understanding and Circumventing the Blood-Brain Barrier, Acta Paediatrica, 92, 83-91, 2003
5 Azevedo,FAC, Carvalho,LRB, Grinberg,LT, Farfel,JM, Ferretti,REL, Leite,REP, Jacob,W, Lent,R, Herculano-Houzel,S. Equal Numbers of Neuronal and Nonneuronal Cells Make the Human Brain an Isometrically Scaled-Up Primate Brain, J.Comp.Neurol., 513, 532-541, 2009
6 Haug,H. Brain Sizes, Surfaces, and Neuronal Sizes of the Cortex Cerebri: A Stereological Investigation of Man and His Variability and A Comparison With Some Mammals (Primates, Whales, Marsupials, Insectivores, and One Elephant, Am.J.Anat., 180, 126-142, 1987
7 Kreczmanski,P, Heinsen,H, Mantua,V, Woltersdorf,F, Masson,T, Ulfig,N, Schmidt-Kastner,R, Korr,H, Steinbusch,HWM, Hof,PR, Schmitz,C. Microvessel Length Density, Total Length, and Length Per Neuron in Five Subcortical Regions in Schizophrenia, Acta Neuropathol.(Berl)., 117, 409-421, 2009
8 Reichel,A. Addressing Central Nervous System (CNS) Penetration in Drug Discovery: Basics and Implications of the Evolving New Concept, Chem.Biodivers., 6, 2030-2049, 2009
9 Pakkenberg,B and Gundersen,HJG. Neocortical Neuron Number in Humans: Effect of Sex and Age, J.Comp.Neurol., 384, 312-320, 1997
10 Karbowski,J. Global and Regional Brain Metabolic Scaling and Its Functional Consequences, BMC Biol., 5, Article 18 2007
11 Abbott,NJ, Patabendige,AAK, Dolman,DEM, Yusof,SR, Begley,DJ. Structure and Function of the Blood-Brain Barrier, Neurobiol.Dis., 37, 13-25, 2010
12 Perge,JA, Niven,JE, Mugnaini,E, Balasubramanian,V, Sterling,P. Why Do Axons Differ in Caliber?, J.Neurosci., 32, 626-638, 2012
13 Lyck,L, Santamaria,ID, Pakkenberg,B, Chemnitz,J, Schroder,HD, Finsen,B, Gundersen,HJG. An Empirical Analysis of the Precision of Estimating the Numbers of Neurons and Glia in Human Neocortex Using a Fractionator-Design With Sub-Sampling, J.Neurosci.Methods, 182, 143-156, 2009
14 Davies,B and Morris,T. Physiological-Parameters in Laboratory-Animals and Humans, Pharm.Res., 10, 1093-1095, 1993
15 Mchenry,LC. Cerebral Blood Flow, N.Engl.J.Med., 274, 82-91, 1966
16 Aanerud,J, Borghammer,P, Chakravarty,MM, Vang,K, Rodell,AB, Jonsdottir,KY, Moller,A, Ashkanian,M, Vafaee,MS, Iversen,P, Johannsen,P, Gjedde,A. Brain Energy Metabolism and Blood Flow Differences in Healthy Aging, J.Cerebr.Blood F.Met., 32, 1177-1187, 2012
17 Koutsiaris,AG, Tachmitzi,SV, Batis,N, Kotoula,MG, Karabatsas,CH, Tsironi,E, Chatzoulis,DZ. Volume Flow and Wall Shear Stress Quantification in the Human Conjunctival Capillaries and Post-Capillary Venules in Vivo, Biorheology, 44, 375-386, 2007
18 Cucullo,L, Hossain,M, Puvenna,V, Marchi,N, Janigro,D. The Role of Shear Stress in Blood-Brain Barrier Endothelial Physiology, BMC Neurosci., 12, 40 2011
19 Aaslid,R, Lindegaard,KF, Sorteberg,W, Nornes,H. Cerebral Autoregulation Dynamics in Humans, Stroke, 20, 45-52, 1989
20 Mota,B and Herculano-Houzel,S. How the Cortex Gets Its Folds: an Inside-Out, Connectivity-Driven Model for the Scaling of Mammalian Cortical Folding, Frontiers in Neuroanatomy, 6, Article 3 2012
21 Herculano-Houzel,S. Scaling of Brain Metabolism With a Fixed Energy Budget Per Neuron: Implications for Neuronal Activity, Plasticity and Evolution, PloS.One., 6, Article e17514 2011
22 Rakusan,K, Flanagan,MF, Geva,T, Southern,J, Vanpraagh,R. Morphometry of Human Coronary Capillaries During Normal Growth and the Effect of Age in Left-Ventricular Pressure-Overload Hypertrophy, Circulation, 86, 38-46, 1992
23 Irons,RD. The Mouse in Biomedical-Research, Vol 3, Normative Biology, Immunology, and Husbandry - Foster,Hl, Small,Jd, Fox,Jg, Am.Sci., 72, 632 1984
24 Edwards,WD and Kitzman,DW. Age-Related-Changes in the Anatomy of the Normal Human Heart, J.Gerontol., 45, M33-M39, 1990
25 Popovic,ZB, Sun,JP, Yamada,H, Drinko,J, Mauer,K, Greenberg,NL, Cheng,YN, Moravec,CS, Penn,MS, Mazgalev,TN, Thomas,JD. Differences in Left Ventricular Long-Axis Function From Mice to Humans Follow Allometric Scaling to Ventricular Size, J.Physiol.Lond., 568, 255-265, 2005
26 Lutgens,E, Daemen,MJAP, de Muinck,ED, Debets,J, Leenders,P, Smits,JFM. Chronic Myocardial Infarction in the Mouse: Cardiac Structural and Functional Changes, Cardiovasc.Res., 41, 586-593, 1999
27 DeMaria,AN, Neumann,A, Lee,G, Fowler,W, Mason,DT. Alterations in Ventricular Mass and Performance Induced by Exercise Training in Man Evaluated by Echocardiography, Circulation, 57, 237-244, 1978
28 Anversa,P, Kajstura,J, Reiss,K, Quaini,F, BALDINI,ALES, Olivetti,G, Sonnenblick,EH. Ischemic Cardiomyopathy: Myocyte Cell Loss, Myocyte Cellular Hypertrophy, and Myocyte Cellular Hyperplasia, Ann.New York Acad.Sci., 752, 47-64, 1995
29 Olivetti,G, Capasso,JM, Sonnenblick,EH, Anversa,P. Side-To-Side Slippage of Myocytes Participates in Ventricular Wall Remodeling Acutely After Myocardial-Infarction in Rats, Circ.Res., 67, 23-34, 1990
30 Henschel,E and Kyrieleis,C. Thermodynamische Messung Äußerer Organoberflächen, Virchows Archiv, 333, 22-28, 1960
31 Vaidya,D, Morley,GE, Samie,FH, Jalife,J. Reentry and Fibrillation in the Mouse Heart - A Challenge to the Critical Mass Hypothesis, Circ.Res., 85, 174-181, 1999
32 Bachner-Hinenzon,N, Ertracht,O, Leitman,M, Vered,Z, Shimoni,S, Beeri,R, Binah,O, Adam,D. Layer-Specific Strain Analysis by Speckle Tracking Echocardiography Reveals Differences in Left Ventricular Function Between Rats and Humans, Am.J.Physiol.Heart, 299, H664-H672, 2010
33 Tibayan,FA, Rodriguez,F, Langer,F, Liang,D, Daughters,GT, Ingels,NB, Miller,DC. Undersized Mitral Annuloplasty Alters Left Ventricular Shape in Acute Ischemic Mitral Regurgitation, Circulation, 108, Suppl.S, 476 2003
34 Indermuhle,A, Vogel,R, Meier,P, Zbinden,R, Seiler,C. Myocardial Blood Volume and Coronary Resistance During and After Coronary Angioplasty, Am.J.Physiol.Heart, 300, H1119-H1124, 2011
35 Brands,J, Spaan,JAE, Van den Berg,BM, Vink,H, VanTeeffelen,JWGE. Acute Attenuation of Glycocalyx Barrier Properties Increases Coronary Blood Volume Independently of Coronary Flow Reserve, Am.J.Physiol.Heart, 298, H515-H523, 2010
36 Schlosser,T, Pagonidis,K, Herborn,CU, Hunold,P, Waltering,KU, Lauenstein,TC, Barkhausen,J. Assessment of Left Ventricular Parameters Using 16-MDCT and New Software for Endocardial and Epicardial Border Delineation, Am.J.Roentgenol., 184, 765-773, 2005
37 Stegger,L, Heijman,E, Schafers,KP, Nicolay,K, Schafers,MA, Strijkers,GJ. Quantification of Left Ventricular Volumes and Ejection Fraction in Mice Using PET, Compared With MRI, J.Nucl.Med., 50, 132-138, 2009
38 Eisele,JC, Schaefer,IM, Nyengaard,JR, Post,H, Liebetanz,D, Brul,A, Muhlfeld,C. Effect of Voluntary Exercise on Number and Volume of Cardiomyocytes and Their Mitochondria in the Mouse Left Ventricle, Basic Res.Cardiol., 103, 12-21, 2008
39 Bersell,K, Arab,S, Haring,B, Kuhn,B. Neuregulin1/ErbB4 Signaling Induces Cardiomyocyte Proliferation and Repair of Heart Injury, Cell, 138, 257-270, 2009
40 Laflamme,MA and Murry,CE. Heart Regeneration, Nature, 473, 326-335, 2011
41 Crescenzi,M. Reactivation of the Cell Cycle in Terminally Differentiated Cells. Landes Bioscience, Georgetown, TX, 2002
42 Lancel,S, Joulin,O, Favory,R, Goossens,JF, Kluza,J, Chopin,C, Formstecher,P, Marchetti,P, Neviere,R. Ventricular Myocyte Caspases Are Directly Responsible for Endotoxin-Induced Cardiac Dysfunction, Circulation, 111, 2596-2604, 2005
43 Nakayama,M, Yan,XH, Price,RL, Borg,TK, Ito,K, Sanbe,A, Robbins,J, Lorell,BH. Chronic Ventricular Myocyte-Specific Overexpression of Angiotensin II Type 2 Receptor Results in Intrinsic Myocyte Contractile Dysfunction, Am.J.Physiol.Heart, 288, H317-H327, 2005
44 Torrance,RW. Allometric Algorithms and the Work of the Heart, Respir.Physiol., 113, 95-99, 1998
45 van der Laarse,WJ. Energetics of Small Hearts, J.Physiol.Lond., 573, 1 2006
46 Janssen,B, Debets,J, Leenders,P, Smits,J. Chronic Measurement of Cardiac Output in Conscious Mice, Am.J.Physiol-Reg.I., 282, R928-R935, 2002
47 Cleveland Clinic Foundation. Cleveland Clinic Heart Book. 1st ed., Topol,EJ, ed. Hyperion, New York, 2000
48 Talley,NJ and O'Connor,S. Examination Medicine: a Guide to Physician Training. 6th ed., Churchill Livingstone Elsevier, Sydney; New York, 2010
49 Gunther,B and Morgado,E. Allometric Scaling of Biological Rhythms in Mammals, Biol.Res., 38, 207-212, 2005
50 Weinberg,PD and Ethier,CR. Twenty-Fold Difference in Hemodynamic Wall Shear Stress Between Murine and Human Aortas, J.Biomech., 40, 1594-1598, 2007
51 Suarez,RK and Darveau,CA. Multi-Level Regulation and Metabolic Scaling, J.Exp.Biol., 208, 1627-1634, 2005
52 Adolph,EF. Quantitative Relations in the Physiological Constitutions of Mammals, Science, 109, 579-585, 1949
53 Calder,WA. Scaling of Physiological Processes in Homeothermic Animals, Annu.Rev.Physiol., 43, 301-322, 1981
54 Prothero,J. Organ Scaling in Mammals - the Kidneys, Comp.Biochem.Phys.A, 77, 133-138, 1984

55 Mordenti,J, Chen,SA, Moore,JA, Ferraiolo,BL, Green,JD. Interspecies Scaling of Clearance and Volume of Distribution Data for 5 Therapeutic Proteins, Pharm.Res., 8, 1351-1359, 1991
56 Beuchat,CA. Structure and Concentrating Ability of the Mammalian Kidney: Correlations With Habitat, Am.J.Physiol-Reg.I., 271, R157-R179, 1996
57 Beuchat,CA. Metabolism and the Scaling of Urine Concentrating Ability in Mammals - Resolution of A Paradox, J.Theor.Biol., 143, 113-122, 1990
58 Edwards,NA. Scaling of Renal Functions in Mammals, Comp.Biochem.Phys.A, 52, 63-66, 1975
59 Calder,WA, III and Braun,EJ. Scaling of Osmotic Regulation in Mammals and Birds, Am.J.Physiol., 244, R601-R606, 1983
60 Singer,MA. Of Mice and Men and Elephants: Metabolic Rate Sets Glomerular Filtration Rate, Am.J.Kidney Dis., 37, 164-178, 2001
61 Boxenbaum,H. Interspecies Scaling, Allometry, Physiological Time, and the Ground Plan of Pharmacokinetics, J.Pharmacokinet.Biopharm., 10, 201-227, 1982
62 Savage,VM, Allen,AP, Brown,JH, Gillooly,JF, Herman,AB, Woodruff,WH, West,GB. Scaling of Number, Size, and Metabolic Rate of Cells With Body Size in Mammals, PNAS (US), 104, 4718-4723, 2007
63 Abrahams,S, Greenwald,L, Stetson,DL. Contribution of Renal Medullary Mitochondrial Density to Urinary Concentrating Ability in Mammals, Am.J.Physiol., 261, R719-R726, 1991
64 Else,PL and Hulbert,AJ. An Allometric Comparison of the Mitochondria of Mammalian and Reptilian Tissues - the Implications for the Evolution of Endothermy, J.Comp.Physiol.B, 156, 3-11, 1985
65 Prothero,JW. Organ Scaling in Mammals: The Liver, Comparative Biochemistry and Physiology Part A: Physiology, 71, 567-577, 1982
66 Boxenbaum,H. Interspecies Variation in Liver Weight, Hepatic Blood-Flow, and Antipyrine Intrinsic Clearance - Extrapolation of Data to Benzodiazepines and Phenytoin, J.Pharmacokinet.Biopharm., 8, 165-176, 1980
67 Booth,J, Boyland,E, Cooling,C. Respiration of Human Liver Tissue, Biochem.Pharmacol., 16, 721-724, 1967
68 Sohlenius-Sternbeck,AK. Determination of the Hepatocellularity Number for Human, Dog, Rabbit, Rat and Mouse Livers From Protein Concentration Measurements, Toxicol.in Vitro, 20, 1582-1586, 2006
69 Couture,P and Hulbert,AJ. Relationship Between Body-Mass, Tissue Metabolic-Rate, and Sodium-Pump Activity in Mammalian Liver and Kidney, Am.J.Physiol-Reg.I., 268, R641-R650, 1995
70 Domansky,K, Inman,W, Serdy,J, Dash,A, Lim,MHM, Griffith,LG. Perfused Multiwell Plate for 3D Liver Tissue Engineering, Lab Chip, 10, 51-58, 2010
71 Lave,T, Dupin,S, Schmitt,C, Chou,RC, Jaeck,D, Coassolo,P. Integration of in Vitro Data into Allometric Scaling to Predict Hepatic Metabolic Clearance in Man: Application to 10 Extensively Metabolized Drugs, J.Pharm.Sci., 86, 584-590, 1997
72 Stahl,WR. Scaling of Respiratory Variables in Mammals, J.Appl.Physiol., 22, 453-460, 1967
73 Hou,C and Mayo,M. Pulmonary Diffusional Screening and the Scaling Laws of Mammalian Metabolic Rates, Phys.Rev.E, 84, Article 061915 2011
74 Stone,KC, Mercer,RR, Gehr,P, Stockstill,B, Crapo,JD. Allometric Relationships of Cell Numbers and Size in the Mammalian Lung, Am.J.Respir.Cell Mol.Biol., 6, 235-243, 1992
75 West,GB, Brown,JH, Enquist,BJ. A General Model for the Origin of Allometric Scaling Laws in Biology, Science, 276, 122-126, 1997
76 Prothero,JW. Scaling of Blood Parameters in Mammals, Comp.Biochem.Phys.A, 67, 649-657, 1980
77 Reference Ranges for Blood Tests, Wikipedia: The Free Encyclopedia Wikimedia Foundation, Inc., 5/1/2012,
78 Kjeld,M and Olafsson,O. Allometry (Scaling) of Blood Components in Mammals: Connection With Economy of Energy?, Can.J.Zool., 86, 890-899, 2008
79 Fernandez,I, Pena,A, Del Teso,N, Perez,V, Rodriguez-Cuesta,J. Clinical Biochemistry Parameters in C57BL/6J Mice After Blood Collection From the Submandibular Vein and Retroorbital Plexus, J.Am.Assoc.Lab.Anim.Sci., 49, 202-206, 2010
80 Arrighi,I, Bloch-Faure,M, Grahammer,F, Bleich,M, Warth,R, Mengual,R, Drici,MD, Barhanin,J, Meneton,P. Altered Potassium Balance and Aldosterone Secretion in a Mouse Model of Human Congenital Long QT Syndrome, PNAS (US), 98, 8792-8797, 2001
81 Reference Values for Laboratory Animals, Research Animal Resources University of Minnesota, 2/19/2013, http://www.ahc.umn.edu/rar/refvalues.html
82 Krauss,GL, Kaplan,P, Fisher,RS. Parenteral Magnesium-Sulfate Fails to Control Electroshock and Pentylenetetrazol Seizures in Mice, Epilepsy Res., 4, 201-206, 1989
83 Greve,JM, Les,AS, Tang,BT, Blomme,MTD, Wilson,NM, Dalman,RL, Pelc,NJ, Taylor,CA. Allometric Scaling of Wall Shear Stress From Mice to Humans: Quantification Using Cine Phase-Contrast MRI and Computational Fluid Dynamics, Am.J.Physiol.Heart, 291, H1700-H1708, 2006
84 Piret,JM and Cooney,CL. Model of Oxygen-Transport Limitations in Hollow Fiber Bioreactors, Biotechnol.Bioeng., 37, 80-92, 1991
85 Roselli,RJ and Diller,KR. Biotransport: Principles and Applications. 1st ed., Springer, New York, 2011
86 Middleman,S. An Introduction to Fluid Dynamics: Principles of Analysis and Design. 1st ed., Wiley, New York, 1998
87 Hartog,A, de Anda,GFV, Gommers,D, Kaisers,U, Verbrugge,SJC, Schnabel,R, Lachmann,B. Comparison of Exogenous Surfactant Therapy, Mechanical Ventilation With High End-Expiratory Pressure and Partial Liquid Ventilation in a Model of Acute Lung Injury, British Journal of Anaesthesia, 82, 81-86, 1999